

**AMES
LABORATORY
IOWA STATE
COLLEGE**

**PROGRESS REPORT ON FRICTION LOSS OF
SLURRIES IN STRAIGHT TUBES**

DISCLAIMER

This report was prepared as an account of work sponsored by an agency of the United States Government. Neither the United States Government nor any agency Thereof, nor any of their employees, makes any warranty, express or implied, or assumes any legal liability or responsibility for the accuracy, completeness, or usefulness of any information, apparatus, product, or process disclosed, or represents that its use would not infringe privately owned rights. Reference herein to any specific commercial product, process, or service by trade name, trademark, manufacturer, or otherwise does not necessarily constitute or imply its endorsement, recommendation, or favoring by the United States Government or any agency thereof. The views and opinions of authors expressed herein do not necessarily state or reflect those of the United States Government or any agency thereof.

DISCLAIMER

Portions of this document may be illegible in electronic image products. Images are produced from the best available original document.

U N C L A S S I F I E D

ISC-474

1
no. 44194

U N I T E D S T A T E S A T O M I C E N E R G Y C O M M I S S I O N

PROGRESS REPORT ON FRICTION LOSS OF SLURRIES IN STRAIGHT TUBES

By

Glenn Murphy, Donald F. Young, and Richard J. Burian

April 1, 1954

Ames Laboratory
at
Iowa State College
F. H. Spedding, Director
Contract W-7405 eng-82

U N C L A S S I F I E D

This report is distributed according to the category Engineering as listed in TID-4500, January 15, 1954.

TABLE OF CONTENTS

	<u>Page</u>
LIST OF SYMBOLS	4
ABSTRACT	6
INTRODUCTION	7
REVIEW OF LITERATURE	8
MATERIALS AND EQUIPMENT	11
A. Materials	11
Size Determination	12
Specific Weight Determination	25
B. Description of Equipment	25
C. Calibration	27
D. Test Procedure	27
ANALYSIS	31
A. Types of Flow	31
B. Prediction of Friction Loss	33
RESULTS	37
DESIGN CONSIDERATIONS	42
CONCLUSIONS	45
LITERATURE CITED	50
ACKNOWLEDGMENTS	51
APPENDIX A	51
Determination of Concentration	51
APPENDIX B	53
Determination of Projected Area of Particles	53
APPENDIX C	58

LIST OF SYMBOLS

The following symbols and subscripts were used in this paper:

<u>Symbols</u>	<u>Units</u>
A_S - effective projected area of solid	ft ²
A_T - total cross sectional area of tube	ft ²
C_S - solids coefficient	
D - diameter of tube	ft
d - diameter of particle	ft
E - transport effectiveness	lb/(sec)(hp)
e - concentration	
f - friction factor	
g - acceleration of gravity	ft/(sec)(sec)
H - head loss	ft
L - length of tube	ft
N - number of particles per disc	
Q - volume rate of flow	ft ³ /sec
q - weight rate of flow	lb/sec
R - Reynold's number	
r - roughness of tube	
V - volume	ft ³
v - velocity	ft/sec
W - weight	lb
w - specific weight	lb/ft ³
α - distribution factor	
ρ - density	slugs/ft ³
μ - fluid viscosity	slugs/(ft)(sec)
ΔP - pressure drop	lb/ft ²

Subscripts

f - fluid
m - mixture

LIST OF SYMBOLS (Continued)

p - individual particle
s - solid
T - tube
L_T - lower transition
U_T - upper transition
w - water

ABSTRACT

This progress report summarizes the ^{are assumptions of} results obtained to date on the experimental evaluation of the loss of head entailed in pumping slurries through a straight horizontal tube. The slurries used in the investigation consisted of spherical particles of glass, steel and lead in water. The particle size and concentrations were nominally constant for a given slurry, but the various slurries tested covered the size range from 0.00122 to 0.0722 inches in diameter. Concentrations from zero to approximately 50 per cent by weight were used.

Three types of flow were observed, each identified by a characteristic distribution of particles across the tube. The high-velocity region is characterized by a uniform distribution of particles; the transition region, by a non-uniform distribution of particles, but no stationary layer; and the low-velocity region, by a stationary layer of particles on the bottom of the tube.

ⁿ Equations were developed for evaluating the loss in head over a range of velocities. _{on}

PROGRESS REPORT ON FRICTION LOSS OF SLURRIES
IN STRAIGHT TUBES

By

Glenn Murphy, Donald F. Young, and Richard J. Burian

INTRODUCTION

The ease with which solids, particularly in the form of particles, may be transported in moving streams of fluid is well known, and certain situations, such as the transportation of silt, sand, and gravel in natural waterways, have been the subject of considerable study. Conservation practices, to reduce the mobility of soil subjected to the force of moving air and water have been developed, and the reverse practice, that of moving quantities of soil, sand, and gravel by jets of water has been used extensively.

While the movement of solids, such as sand, cement, coal, grain and other materials by blowing them in air or water through a pipe line is recognized commercially as a standard materials-handling technique very little has been published concerning the laws governing the phenomenon. Consequently, little is known regarding the optimum handling conditions.

The possibility of utilizing a slurry fuel for a nuclear reactor by pumping a suspension of fuel particles in a suitable fluid through the core of the reactor, and perhaps through a heat exchanger as well, is an example of an application in which accurate information concerning the optimum transportation conditions is imperative. For virtually all of the commercial applications indicated, the problem is one of moving the maximum amount of solids at a given or minimum power requirement. In general, more information than now appears in the literature is required on the following items:

- a. The velocity required to prevent settling of the particles.
- b. The velocity required to maintain a uniform distribution of solids.
- c. The velocity at which the most economical operation is obtained.
- d. The optimum particle size.
- e. The optimum concentration.
- f. The loss in head, or power required to overcome friction.

In addition, more information is needed on the erosion-corrosion effects, the heat transfer properties, and the best types of pumps for handling slurries, or solid-fluid mixtures.

This report presents the results obtained in one phase of an investigation of the transportation characteristics of slurries. It is directed primarily toward the evaluation of the loss of head in a straight horizontal tube of circular cross section, through which are pumped solid-fluid mixtures. In the tests reported herein concentrations up to 50 per cent by weight of solid to weight of mixture were studied. Glass, steel, and lead particles were used, having diameters ranging between 0.0012 in. and 0.0722 in. Thus, all particles were above the colloidal range in size. The fluids used in the tests reported here were water and a sodium hydroxide solution.

REVIEW OF LITERATURE

In reviewing the work done by previous investigators it was found that little information was available on the general laws governing the flow characteristics of suspensions. Much of the earlier work had been directed toward the study of the flow of sand and gravel in pipe lines. Although these specific materials are not of primary interest here, a summary of the conclusions drawn from some of the more outstanding investigations may be of interest.

One of the earliest investigators studying the flow of suspensions was Nora Stanton Blatch (3). In connection with the design, construction, and operation of a sand filtration plant for the purification of the public water supply of Washington, D.C., Miss Blatch performed a set of experiments to obtain information on the flow of sand and water in pipes under pressure. The experiments were carried out in a 1-in. diameter brass pipe and in a 1-in. diameter galvanized-iron pipe using two sizes of sand. One sand passed 20-mesh and was retained on 40-mesh sieve, and the other sand passed 60-mesh and was retained on 100-mesh sieve. The specific gravity of both sands was 2.64. The experimental equipment was set up in such a manner that the velocity and concentration of sand could be controlled. Head loss versus velocity data were obtained for different concentrations.

From her experimental work Miss Blatch gave the following conclusions for the conditions under which the experiments were performed (3, p. 407):

1. Two distinct conditions of flow exist: one is obtained for velocities less than about 3 1/2 to 4 feet per second (fps), and the other for velocities above 4 to 10 fps. Between these two conditions of flow is a transition range which is short if the sand is fine and uniform, and long if the sand is graded.

2. The total loss of head due to any given mixture of sand and water is almost constant for low velocity flow, for the transition period it increases with a lower power of the velocity than the loss of head due to water alone (that is less than the 1.7^4 power of the velocity), and for high-velocity flow, the indications seem to be that the loss of head increases with a higher power of the velocity than 1.7^4 .
3. The excess loss of head, over that when water alone is flowing, is greatest for low velocities and least just where high velocity flow sets in.
4. The loss of head due to fine sand for any given percentage and velocity below about 7 fps is less than that due to coarse sand. For higher velocities the loss of head seems to be greater for the fine sand.
5. The total loss of head is greater at all velocities for the galvanized-iron than for the brass pipe.
6. Since the loss of head, due to any given mixture of sand and water, for both grades of sand and both kinds of pipe, is least at a velocity of from 3 to 4 fps, about $3 \frac{1}{2}$ fps is the most economical velocity for a 1-in. pipe. (Economical velocity is that at which the loss of head due to any given mixture of sand and water is a minimum.)
7. At any given velocity, the higher the percentage of sand the more economical is the process.

Short glass sections were inserted in both kinds of pipe so that the nature of the flow could be observed directly. It was found that at velocities below the transition region the greater part of the sand was dragged along the bottom of the pipe at a low velocity, with practically clear water flowing in the upper part of the cross section. At about the economical velocity large quantities of sand began to be carried in suspension. At the higher velocities, all of the sand was carried in suspension throughout the cross section. From these observations it was concluded by Miss Blatch that the high head loss at low velocities was due to the dragging of the sand along the bottom of the pipe and to the small cross section available for the flow of water. The gradual decrease in the head loss during the transition period as the velocity increased was due to the gradual suspension of the sand. At high velocities the loss of head due to the sand is small because all the sand is suspended.

M. P. O'Brien and R. G. Folsom (8) performed a set of experiments on the transportation of sand in pipe lines. In their investigation two sizes of wrought iron pipe (2 in. and 3 in.) and several different types of sands were used. The data were confined chiefly to higher velocities and the principal results drawn from the investigation were: (1) above some

velocity, the head loss in any given pipe line is the same as would occur with clear water at the same mean velocity, and (2) the pressure drop increases in proportion to the specific gravity of the suspension.

Also included in this paper was a discussion of some of the theoretical aspects of the flow of suspensions. One phase of this investigation was concerned with the effects of solids on turbulent flow and the following is a brief summary of the discussion.

Turbulent flow with material in suspension cannot be regarded as identical with flow of the same fluid without solids in the same pipe and at the same mean velocity for a number of reasons. The principal differences are these:

1. The settling particles tend to drag the surrounding fluid with them and to alter the fluctuations in velocity.
2. In a circular pipe the particles tend to fall to the lowest point and hence the concentration of the material may not be the same throughout the cross section.
3. As the particles settle relative to the surrounding fluid each particle induces turbulence of its own which is added to the general turbulence of the flow.
4. In striking the walls the solid particles tend to break up the laminar sub-layer. This effect is possibly greatest near the bottom of the pipe.

H. E. Babbitt and D. H. Caldwell (1,2) performed two series of experiments in studying the flow characteristics of sludges pumped through circular pipes. The laminar flow of sludges was first studied with special reference to sewage sludge. It was assumed that the flow of sludges obeyed the fundamental formula for true plastics and a theoretical equation was developed for predicting the head loss. The equation was written in terms of velocity, pipe diameter, density of sludge, yield value of sludge, and coefficient of rigidity. This equation was checked against experimental data and gave agreement that was considered satisfactory by the authors. The second series of tests performed by Babbitt and Caldwell was concerned with the turbulent flow of sludges. It was found that above some critical velocity the head loss could be determined from the conventional Darcy formula ($H = f \frac{L}{D} \frac{v^2}{2g}$), in which f was a friction factor which was determined experimentally.

G. W. Howard (5) performed experiments on the transportation of sand and gravel in a four-inch pipe. Two separate series of tests were performed, each on a different material and each for a range of velocities and concentrations. The two materials tested were Pearl River sand (diam. range 0.0004 in. to 0.08 in.)

and a coarser sand (up to 0.25 in. diam.). From the experimental data equations of the form $H_f = mv^x$ were developed for the flow above the transition region. Equations for m and x in terms of the concentration were also given. The following conclusions were drawn by Howard (5, pp. 1389-90).

1. Sand is transported in pipes by rolling along the bottom at low velocities, "jerking" along the bottom at medium velocities, and by having all particles in motion at velocities greater than the range in which "jerking" occurs.
2. The largest quantity of material is transported in the lower third of the pipe rather than along the bottom.
3. For pipes carrying sand, values of f in the Darcy formula decrease with an increase in velocity.
4. Values of f increase with an increase in solid concentration, for any velocity.
5. A general formula for use in determining head loss in pipes carrying sand is definitely not satisfactory for use by any person who has not had considerable experience with the use of the formula.
6. The economical velocity for transporting solids depends upon the character of the material to be carried, and each class of material will probably have a different economical velocity for the same size of pipe.
7. A pipe line, transporting material of a large grain size at low velocities, will become blocked much more frequently than pipes carrying material of a small grain size, because the larger particles tend to become locked, obstructing other particles, and do not form a smooth bed over which the material can be moved.
8. The transfer of results from a small pipe line to a line of greater diameter must be qualitative and not governed by any law of corresponding velocities.

Additional sources for literature in this field can be found in two bibliographies entitled "Mechanical Characteristics of Slurries," by Murphy, Mitchell and Young (6,7).

MATERIALS AND EQUIPMENT

A. Materials

Glass, lead and steel spherical particles were selected for the solid phases of the slurries and tap water, as the liquid

component in the majority of the tests. A few check runs were made using an NaOH solution. The lead particles were shot with an average diameter of 0.0505 in. Two sizes of steel shot, 0.0149 and 0.0722 in. diam and four sizes of glass spheres were used. These latter included spheres of 0.0020, 0.0026, 0.0114, 0.0314 in. diameters. In addition a smaller size (av diam 0.0012 in.) of glass particles was obtained by grinding some of the 0.0020-in. particles in a ball mill.

Size Determination

With one exception, two methods were used in obtaining the average diameter of the particles. In one method actual measurements were made of a number of the particles under a microscope which had a traveling eye piece. For the second method photographs were taken of the particles and measurements taken from the photographs. The latter method gave both the size and appearance of the particles. Representative samples of the particles before the test and after the test were obtained and these samples were reduced by quartering until the quantity of particles was small enough to be mounted on a standard microscope specimen slide. This was accomplished by dispersing the particles in Canada balsam. The slides were photographed using a standard camera attachment for the microscope. The magnification was determined from a photograph taken of a specimen of known size at the same camera and microscope setting that was used in photographing the particles. The specimens used for this purpose were small lengths of wire (Karma alloy wire and copper wire) whose diameters were determined using a monocular microscope and checked using a micrometer.

The sizes were obtained by actual measurements on the photographs. For Figs. 1 through 7 and 9 through 11 (which are sample photographs) two measurements were taken of each particle, one on the horizontal diameter and the other on the vertical diameter. In Figs. 6 and 7 it was observed that many of the particles were oblong in shape. In determining the size of these particles measurements were taken along the major and minor axis. The average diameter was determined as the arithmetic average of the measurements. Fig. 8 is a photograph of the "ground" glass particles. Their average size was determined by the hydrometer method.

The sizes were determined from the photographs labeled "as-run." The particles classified "as-run" were those taken from a sample obtained at the completion of the tests. In order to determine whether or not there was any appreciable change in the shape of the particles during the experiments, photographs were taken of the particles in their original condition. By comparing these with the photographs taken after the runs it appeared that there was little breaking up of the particles during the course of the experiments. As stated in the procedure, the 0.0020-in. and the 0.0026-in. particles were pumped as a suspension directly through the pump with no apparent damage. It was also observed that with the exception of the ground glass most of the particles were approximately spherical in shape with very few sharp edges appearing.

13

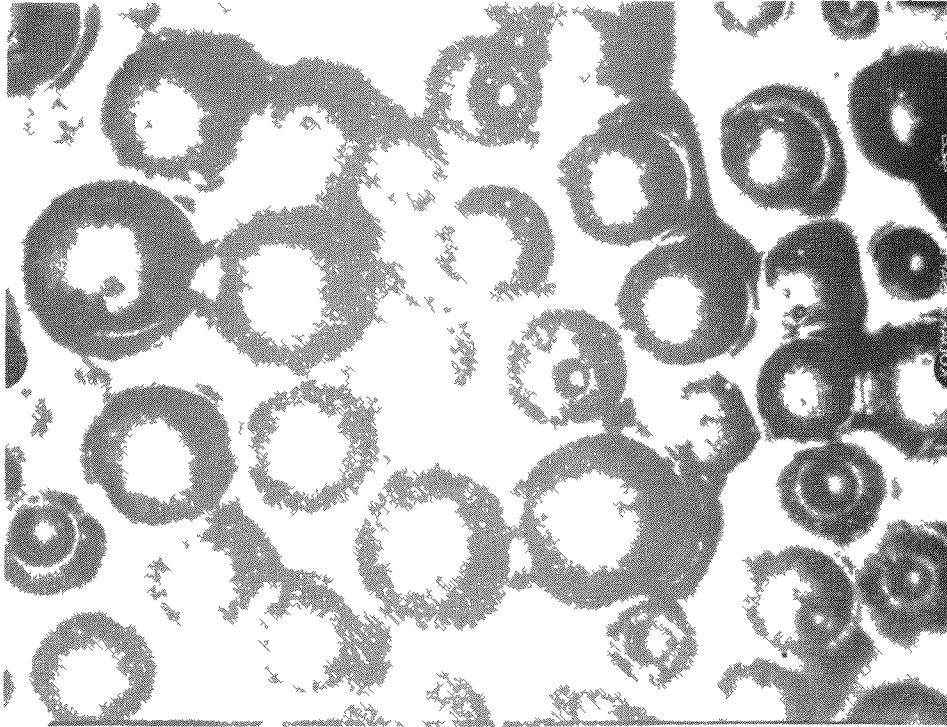


Fig. 1 - As-run glass particles, average diameter 0.0020 in.
(Magnification 293:1).

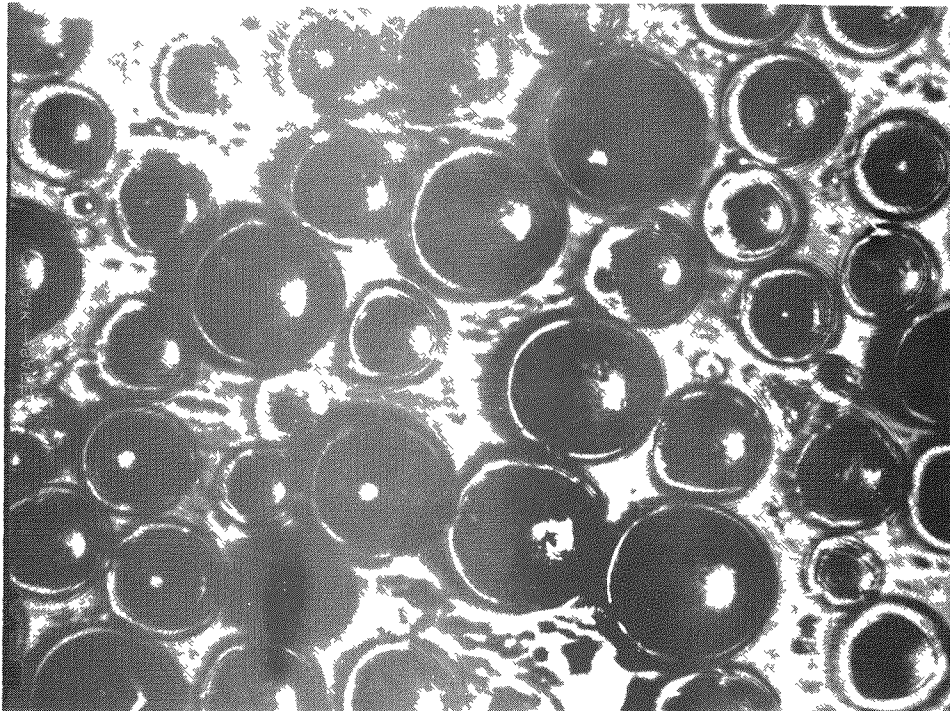
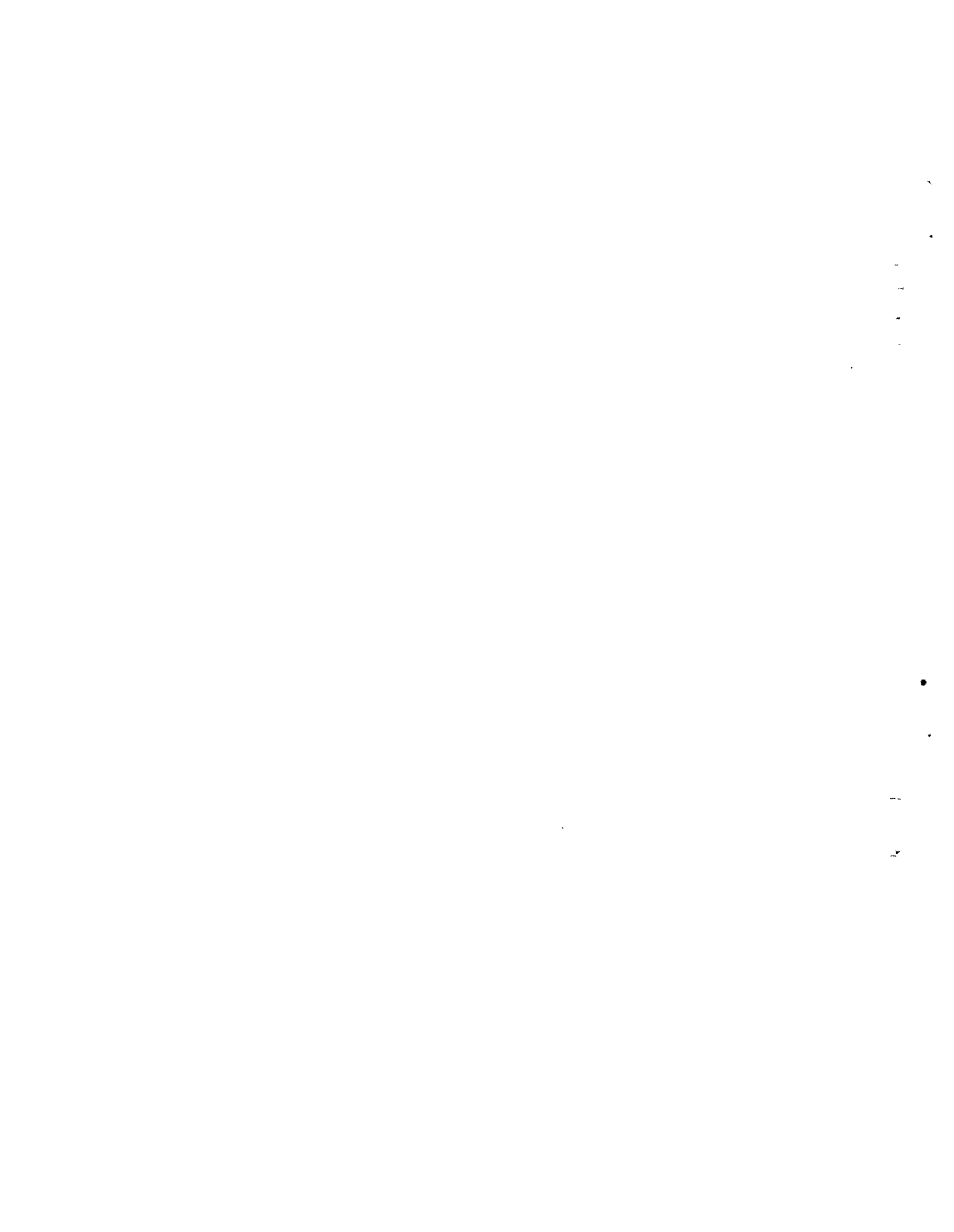


Fig. 2 - 0.0020 in. glass particles before test (Magnification
541:1).

14



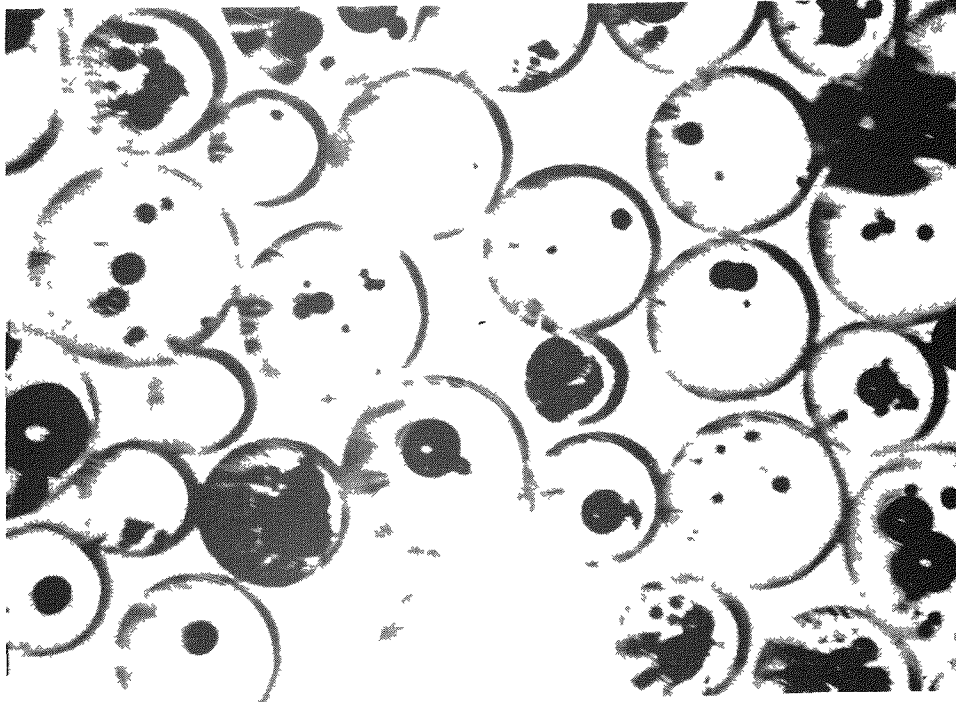


Fig. 3 - As-run glass particles, average diameter 0.0026 in.
(Magnification 318:1).

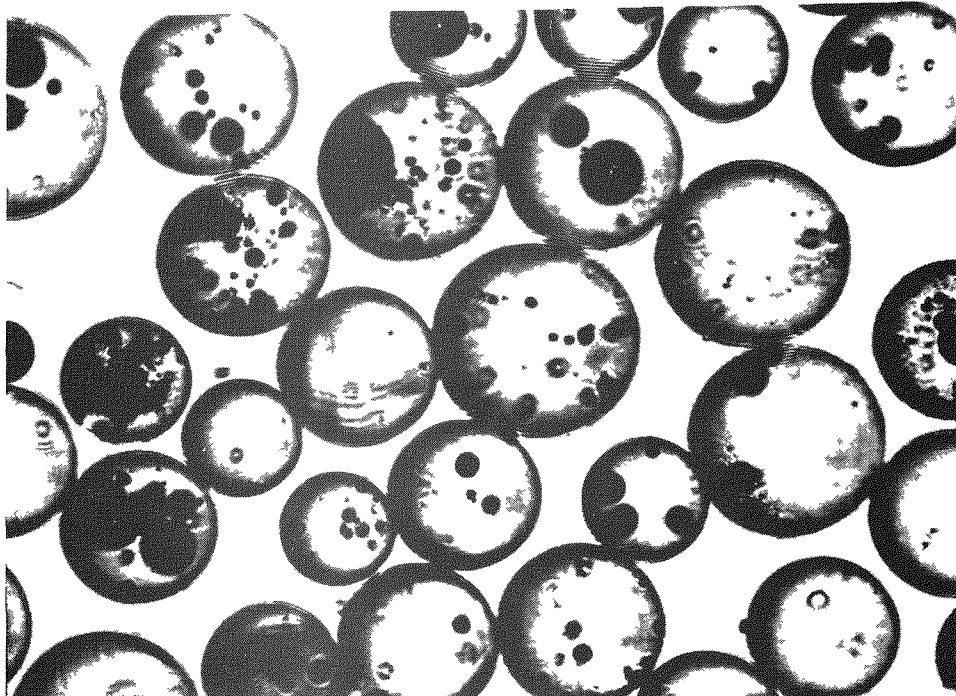


Fig. 4 - 0.0026 in. glass particles before test (Magnification
328:1).

16

1
2
3
4
5

6
7

8
9

17

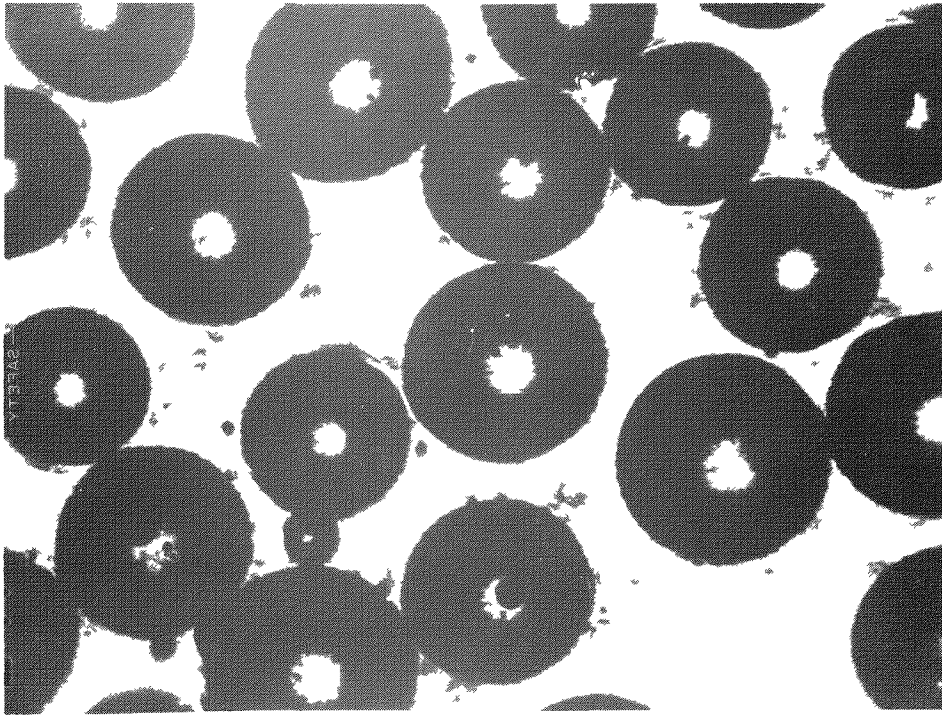


Fig. 5 - As-run glass particles, average diameter 0.0114 in. (Magnification 86.:1).

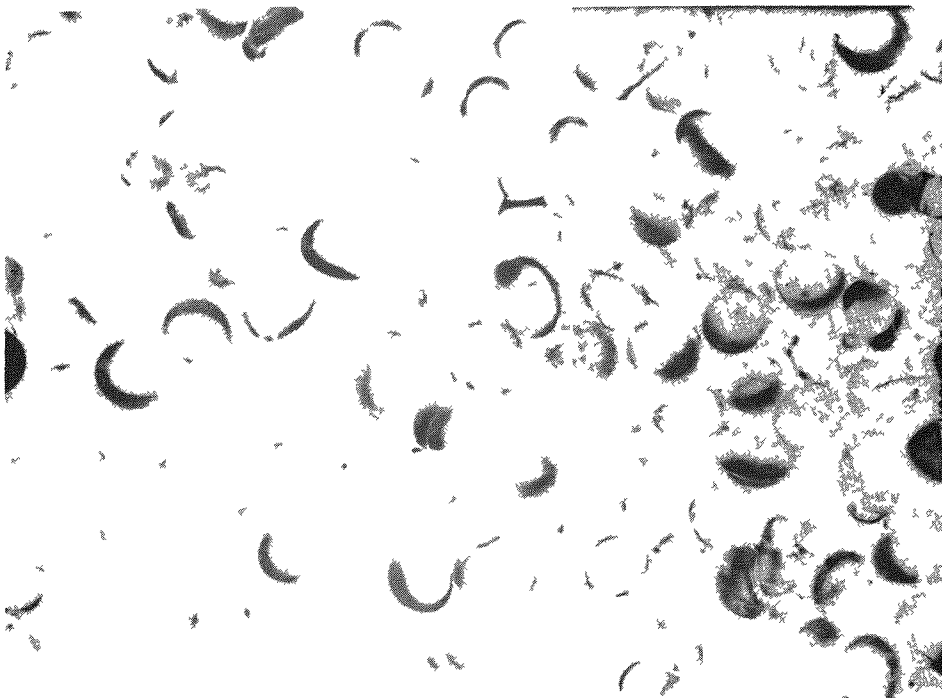


Fig. 6 - As-run glass particles, average diameter 0.0314 in. (Magnification 11.6:1).

18

1
2
3
4

5
6
7
8

19



Fig. 7 - 0.0314 in. glass particles before test (Magnification 11.6:1).

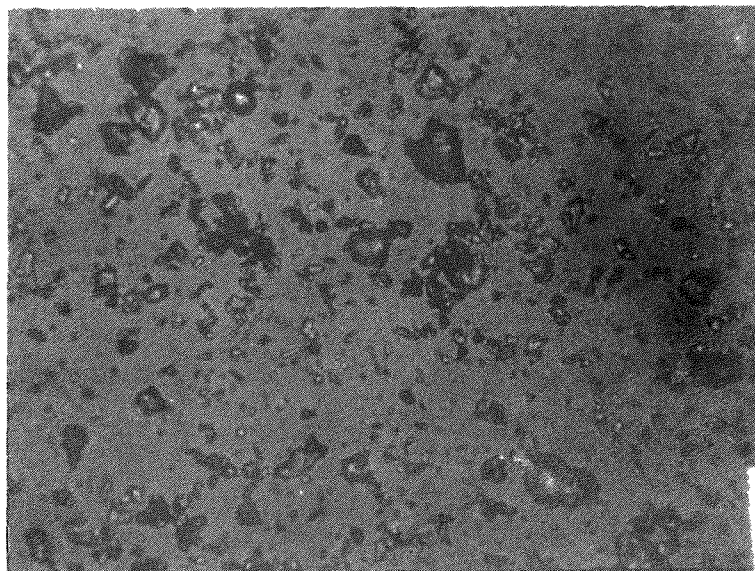


Fig. 8 - As-run ground glass particles, average diameter 0.0012 in.

20

1
2
3
4
5

6
7
8
9
10

21

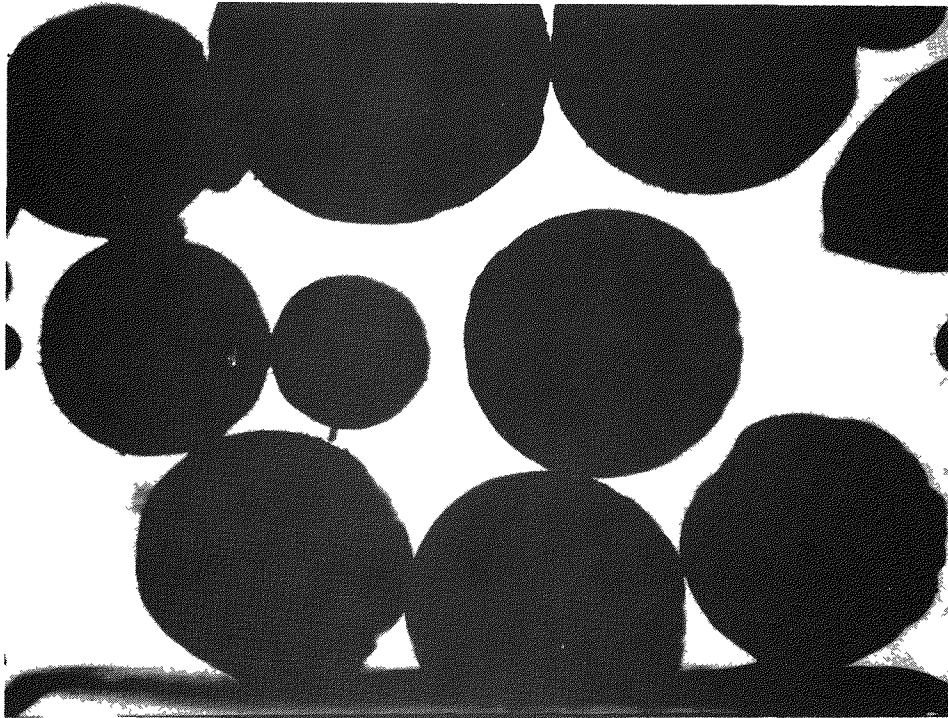


Fig. 9 - As-run steel particles, average diameter 0.0149 in.
(Magnification 82.7:1).

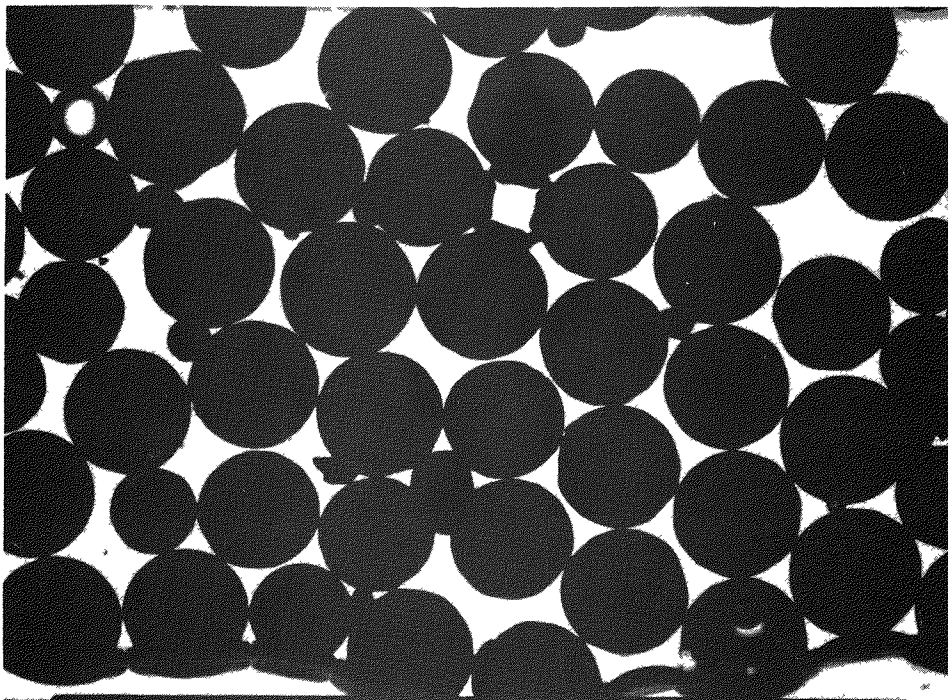


Fig. 10 - As-run lead particles, average diameter 0.0505 in.
(Magnification 12.4:1).

22



23

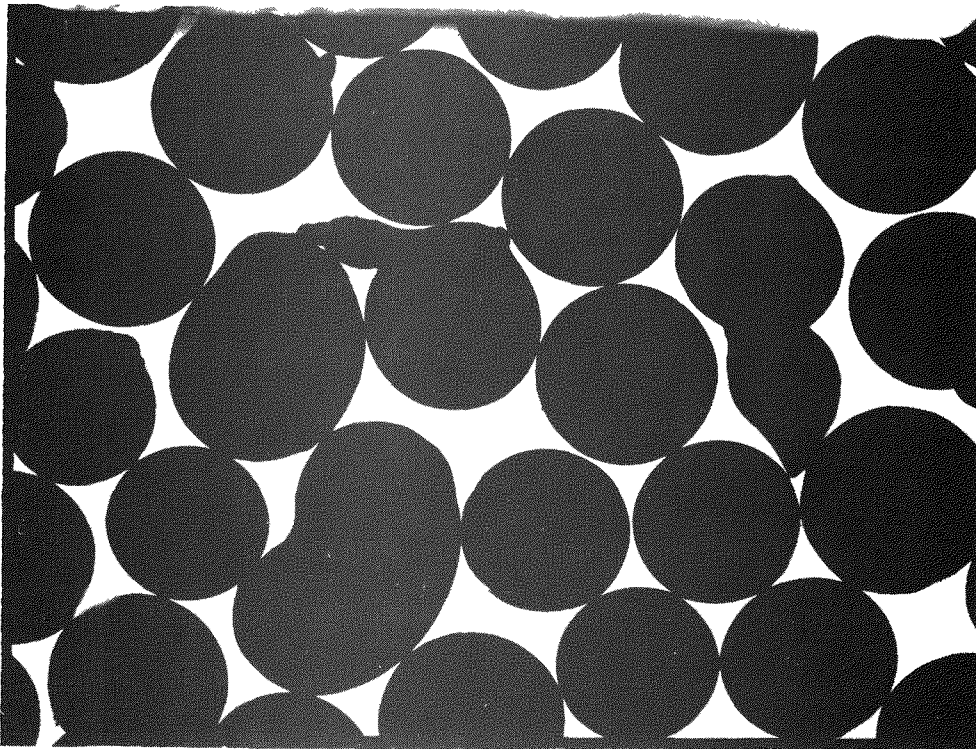


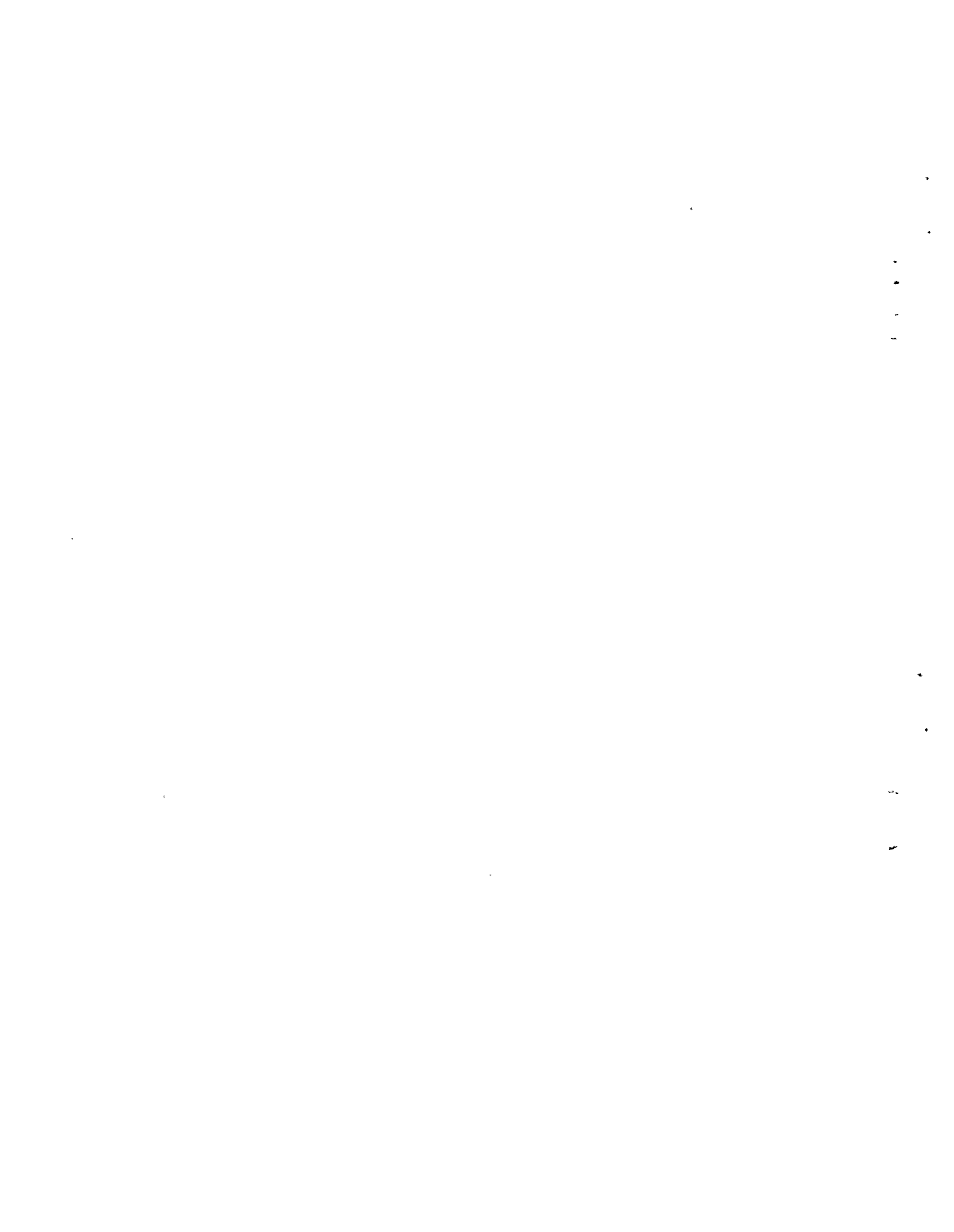
Fig. 11 - As-run steel particles, average diameter 0.0722 in.
(Magnification 12.1:1).

Table I contains a summary of the size determinations.

Table I

Particle Size and Specific Weight

Material	Average Diameter in.	Minimum Diameter in.	Maximum Diameter in.	Specific Weight lb/ft ³
Glass (ground)	0.00122	-----	-----	146.4
Glass	0.0020	0.0010	0.0033	146.4
Glass	0.0026	0.0015	0.0035	174.2
Glass	0.0114	0.0091	0.0136	177.9
Glass	0.0314	0.0215	0.0474	156.9
Steel	0.0149	0.0100	0.0199	465.0
Steel	0.0722	0.0612	0.0812	471.0
Lead	0.0505	0.0373	0.0598	705.0



Specific Weight Determination

The specific weight of the particles was determined by a differential weight and volume method. The particles were added to a definite volume of a known fluid while it was simultaneously stirred to remove air bubbles. The differences between the initial and final weights and volumes gave the total weight and volume of the particles, from which the specific weight was determined. Two fluids were used in these determinations, carbon tetrachloride and water. Table I contains a summary of the results.

B. Description of Equipment

The equipment used in the experiments included the test section, pump and motor unit, water supply tank, solids feed tanks, measuring tank, scales, and two differential manometers. A schematic diagram of the experimental set-up is given in Fig. 12.

Because of a limited amount of space available for the apparatus a relatively short test section was used, thus making it necessary to use a tube of small diameter in order to obtain appreciable head losses. A glass tube was selected as it permitted visual observation of the flow. The average inside diameter of the tube was 0.496 in. The over-all length of tubing was approximately 12 ft with an inclined return section of approximately the same length. Both the test section and return section were mounted on a wooden frame.

In order to maintain a constant head on the pump a supply tank (A) was put in the system. This tank had a capacity of 2.9 cu ft and was supplied with water from an outside source (E). A notch (V) was cut on the top of tank to take care of the overflow and to keep the water at one level during the tests. The outside supply of water was varied to offset the water being pumped. A baffle plate was put in the tank to help quiet the water before entering the suction line. The suction line was directly connected to the pump from the supply tank. Two pumping units were used during the tests. The first was an Oberderfer centrifugal pump (N) with which a velocity of 10 fps in the test section was reached. Since higher velocities were desired a larger unit was installed. This unit consisted of a Worthington centrifugal pump with a 5 hp motor. With the larger unit velocities of 15 fps were obtained. The set-up for the smaller unit is shown on the diagram.

Between the pump and the test section the solid particles were injected into the moving stream at a point (W) directly below the solids feed tank (C). A feed control valve (shown in a detail on Fig. 12) was used to inject the solids at a constant rate. The solids feed tank was under pressure and the rate of discharge of the solids could be controlled by varying the pressure in the tank and by adjusting the position of the feed control valve at (G). The solids feed tank, which had a capacity of 1.3 cu ft, was loaded manually after each series of tests.

26

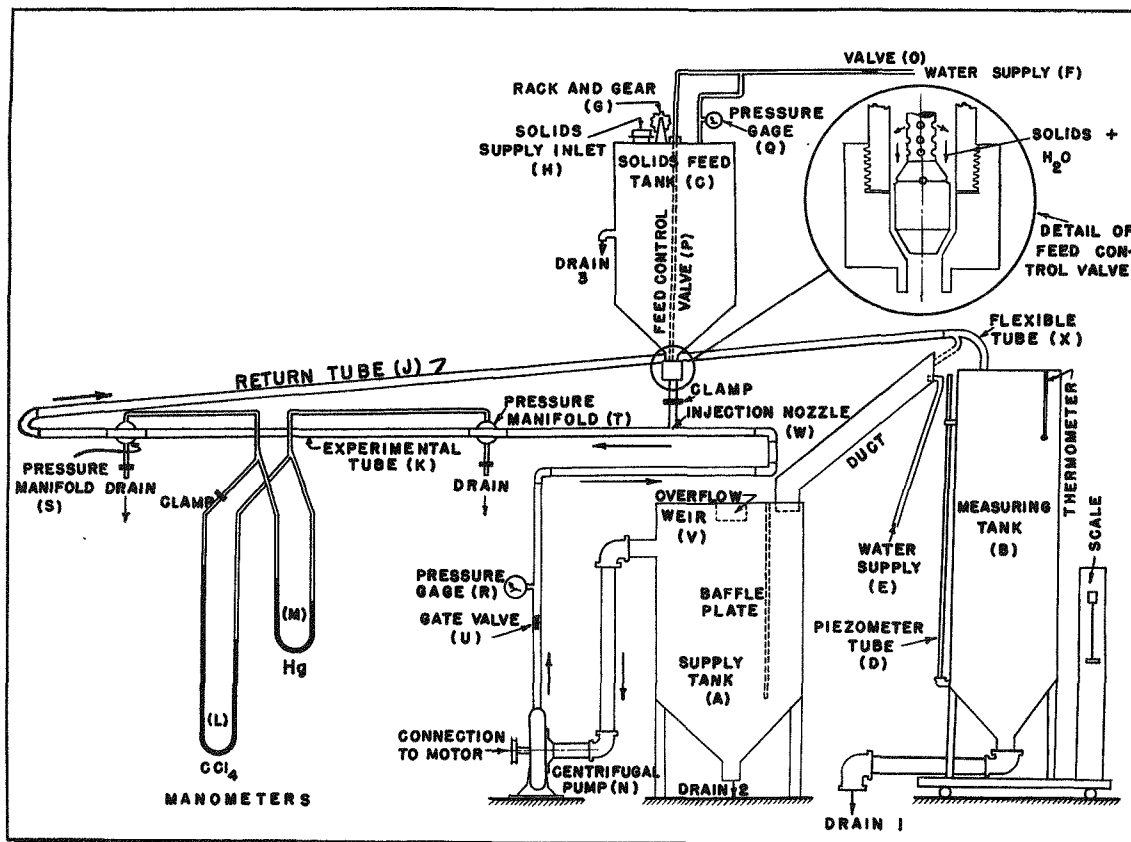


Fig. 12 - Schematic diagram of flow equipment.

The actual test section which was 46 in. long started 43 in. downstream from the point of solids injection. The manometers (L,M) were connected to the test section through two pressure manifolds (S,T). Two differential manometers connected in parallel were used, one filled with colored carbon tetrachloride and the other with mercury. By using the two manometers with different gage fluids, a large range of head losses could be measured with sufficient accuracy.

A draining valve was included on each pressure manifold to permit removal of the fine particles which settled through the holes in the manometer connections during a run.

After passing the test section the suspension moved through the return tube (J) into either the supply tank or the measuring tank (B), depending on the position of the flexible hose (X) at the end of the return tube. Before the test run actually began the suspension was directed into the supply tank and at the beginning of the test run the flow was switched into the measuring tank. This tank had a capacity of 2.5 cu ft. Connected directly to this tank was a piezometer tube (D) with which the volume of the mixture was obtained. The measuring tank was mounted directly on a Fairbanks beam balance scale from which the weight was obtained. Figures 13 and 14 are photographs of the equipment.

Auxiliary pieces of equipment used were a mercury thermometer and a stop watch which could be read to the nearest tenth of a second. The pump connections were made with galvanized-iron pipe and all flexible connections in the apparatus were made with Tygon tubing.

C. Calibration

After the equipment had been constructed and placed in working order it was thought advisable to check the pressure connections against some known values. This was accomplished by running tests with clear water in the laminar flow region. In this region the head loss could be determined using the Hagen-Poiseuille equation:

$$H = \frac{v^2}{2g} \frac{L}{D} \left(\frac{64}{R} \right). \text{ Since the head losses to be measured were small,}$$

a differential inclined manometer was used to measure the pressure drop. Head loss data were obtained in both the laminar and turbulent range and the data compared with known values. Figure 15 shows a plot of friction factor versus Reynolds Number with curves for comparative data drawn in.

D. Test Procedure

For the performance of a test a definite basic procedure was followed for each run. This standardized procedure was necessary since many operations had to be performed during each test run. The following outline summarizes the basic test procedure in the correct sequence.

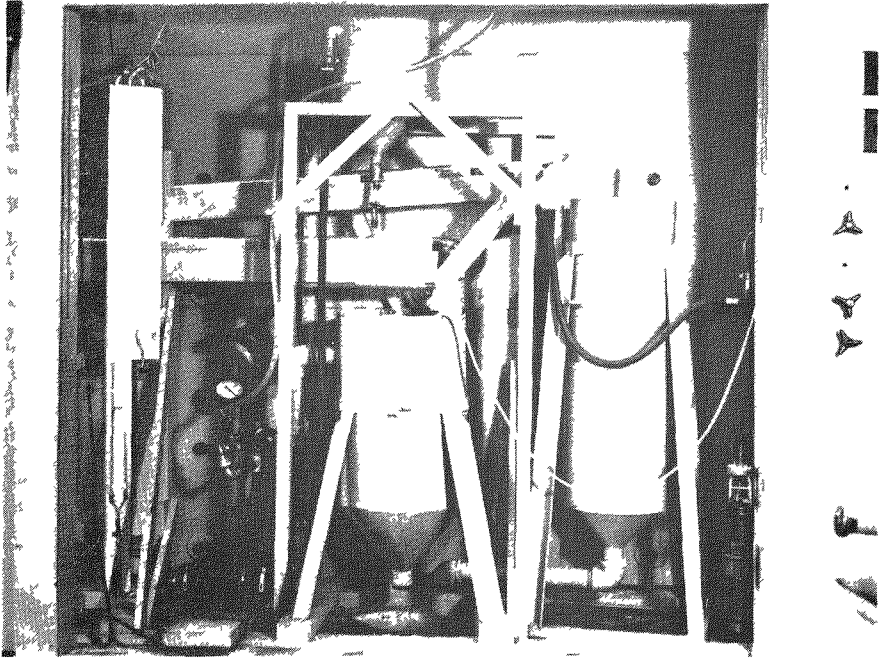


Fig. 13 - Close-up of major items of equipment.

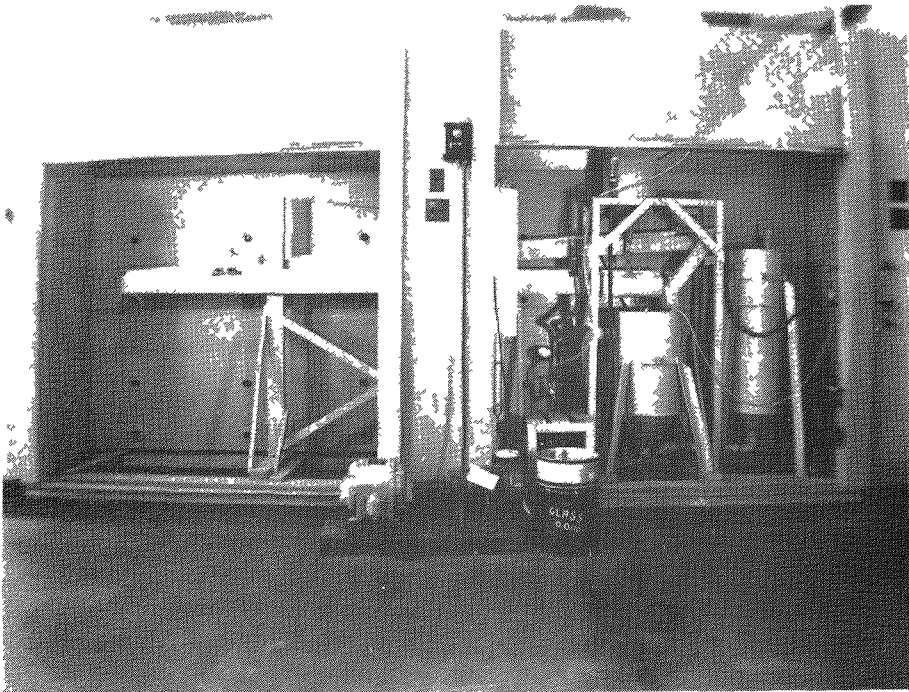


Fig. 14 - Experimental equipment used in slurry tests.

1. The solid particles were loaded manually into the solids feed tank and the tank was then filled with water and sealed. All air was bled from the tank. The bleeding of air was necessary in order to obtain a constant flow of particles.
2. The scales were balanced, the water supply turned on and the water supply tank filled to capacity.
3. The pump was primed, if necessary, and put into operation. The water supply was adjusted for the quantity of flow required for a particular test so that a constant head was maintained in the supply tank. The manometer lines were bled of air.
4. With the fluid being directed back into the supply tank from the return tube, the clamp on the hose between the solids feed tank and the injection nozzle was opened and the pressure in the solids feed tank adjusted to give the concentration desired. The concentration could be determined approximately by the use of a 500 ml graduated cylinder and a small set of scales. With the suspension flowing in the system a quantity of the mixture was directed into the graduated cylinder and the volume and weight determined. From these readings the specific weight of the mixture was calculated and the concentration flowing in the system determined (see Appendix A) from a plot of concentration versus specific weight.
5. After the system had reached an equilibrium condition the actual test was started by switching the flow from the supply tank into the measuring tank. The stop watch was started simultaneously with this movement.
6. The following data were taken during the test run: manometer reading, temperature of mixture, and visual observation of the flow. When possible, several readings of the above mentioned data were taken and the average value recorded. Also during the run, if possible, the concentration was checked by the method outlined in step 4. This section was taken as a check against possible variation in the concentration during a run.
7. As the beam on the scales passed its balance point the flow was switched from the measuring tank into the supply tank and the watch stopped simultaneously. The scale reading, the piezometer reading, and the time were recorded.
8. After the data had been recorded, the measuring tank was emptied into a container by pulling the plug in the bottom of the tank. The particles were reloaded into the solids feed tank if necessary. The number of runs which could be obtained with one loading varied, and depended upon the quantity of flow and concentration. During the reloading period the particles which had accumulated in the water supply tank (in the period before the test began) were also loaded into the solids feed tank.

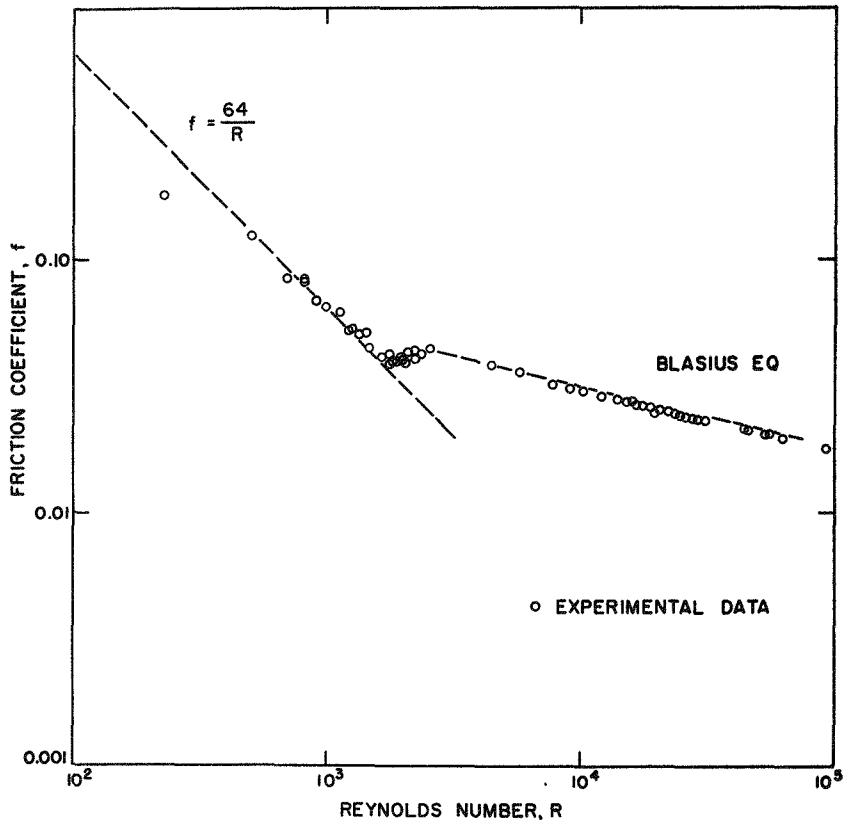


Fig. 15 - Correlation data for experimental equipment.

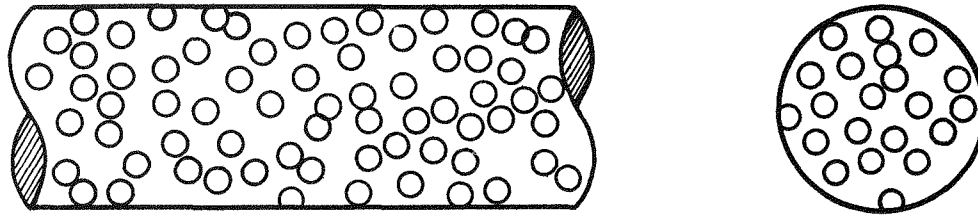
The majority of the tests were run at a temperature of approximately 15 C but several series of tests were run at elevated temperatures of approximately 30 C and 50 C and at a low temperature of approximately 3 C. The water supply for the high temperature test was obtained directly from the hot water line of the outside source. The low temperature was obtained by adding ice to the water supply tank and the solids feed tank. For tests other than those at 15 C some difficulty was encountered in maintaining a constant temperature during the test run.

In working with the spherical fine particles (diameter of 0.0020 in. and 0.0026 in.) and the ground glass particles, a difficulty arose due to the increase in the time which was necessary for the particles to settle. When the particles were drained from the measuring and supply tanks into the container used in loading, the particles had to settle out and leave only fluid on top (which could be poured off) in order to facilitate loading. Another problem that arose was maintaining a constant concentration of the fine particles during a test run. The problem was due to the erratic feeding from the solids feed tank. The solution to both of these problems was thought to be in the altering of the experimental set-up so that the suspension could be mixed directly in the supply tank and pumped as a mixture. By using this method the desired concentration could be mixed in the supply tank, thereby eliminating the variation due to erratic feeding from the solids feed tank. This system also facilitated the loading since the solids and suspension did not have to be separated but the mixture could be transferred directly back into the supply tank. One difficulty arising with this set-up was the rise in temperature due to the recirculation of the mixture. A small cooling coil was added to help maintain a constant temperature. The only additional piece of equipment necessary for pumping the suspension directly through the pump was a mixer.

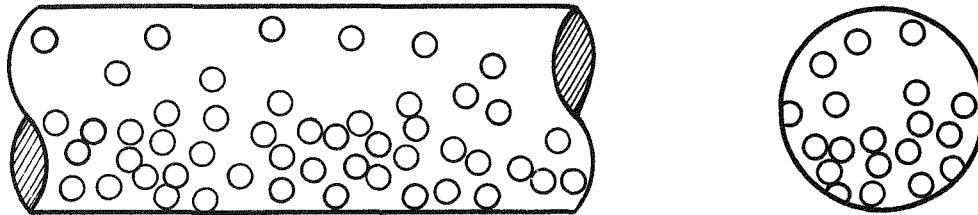
ANALYSIS

The mixer used was an Industrial Mixer (with a 1/30 hp motor, a 15 in. shaft, and a 3 in. propeller), which could be clamped onto the supply tank. This setup was used in obtaining the data for the 0.0020-in. diameter particles, ground glass and for part of the data for the 0.0026-in. diameter particles. In comparing the data taken by the original setup (using solids feed tank) with that taken using the mixer, no discrepancies were observed for the 0.0026-in. particles. velocity diagram.

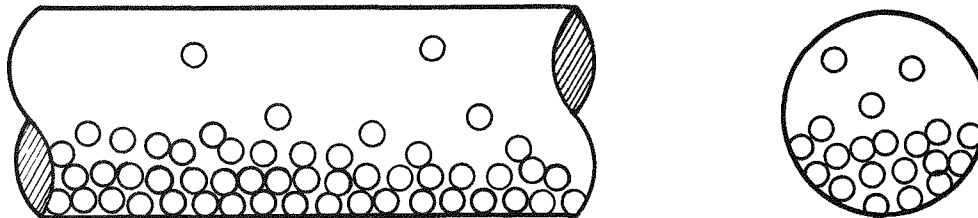
The three characteristic types of distribution are indicated in Fig. 16 and are designated as the high velocity region, the transition region, and the low velocity region. The high velocity region is characterized by an approximately uniform distribution of solids throughout the pipe; the transition region, by a non-uniform distribution of solids but no stationary layer of particles; and the low velocity region by a stationary layer of particles in the pipe. The lower limit of the high velocity region (the minimum velocity at which the solids are uniformly distributed) is called the upper transition velocity and the velocity at the



A. HIGH VELOCITY REGION - UNIFORM DISTRIBUTION



B. TRANSITION REGION - NON-UNIFORM DISTRIBUTION (NO STATIONARY LAYER)



C. LOW VELOCITY REGION - NON-UNIFORM DISTRIBUTION (STATIONARY LAYER)

Fig. 16 - Sketches illustrating three characteristic distributions.

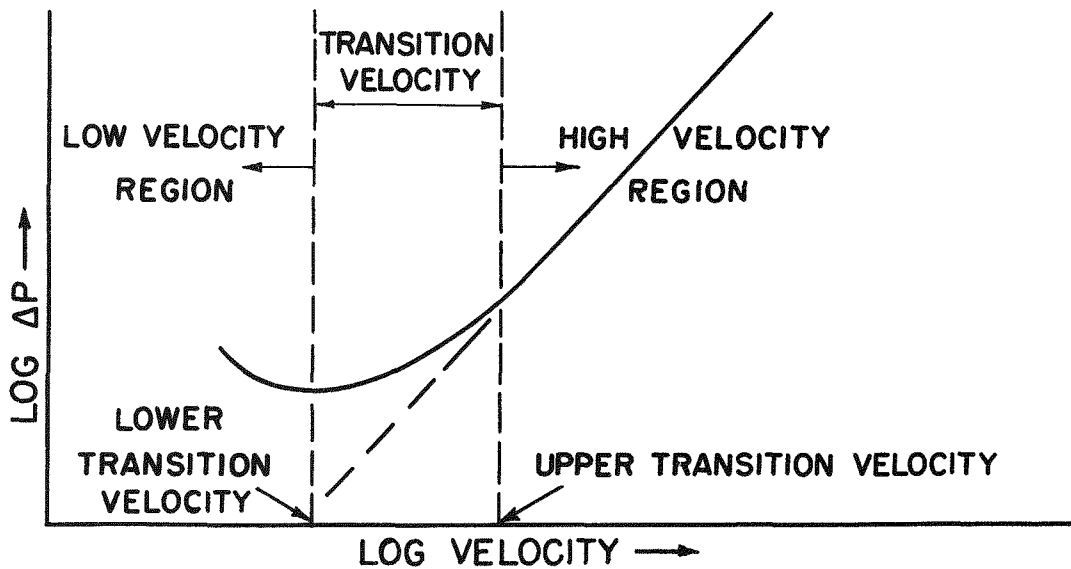


Fig. 17 - Sketch locating different regions of flow.

minimum head loss is the lower transition velocity (the upper limit of the low velocity region). The lower transition velocity corresponds to the velocity at which a stationary layer of particles is formed. Figure 17 shows the approximate location of the various regions of flow on a typical $\Delta P-v_m$ curve.

B. Prediction of Friction Loss

A rigorous analysis of the friction loss developed by a liquid-solid mixture being pumped through a straight pipe of constant diameter is difficult because of the random motion of the particles and the liquid under the condition of turbulent flow that will generally prevail. The analysis may be simplified by assuming laminar flow, but it is known that for a liquid alone the actual loss in head is appreciably greater under the condition of turbulent flow than under the condition of laminar flow. The added energy required to overcome the added loss in turbulent flow is attributed to the greater relative motion between particles. Young (9) has analyzed the laminar flow structure in a system composed of annular rings of solid particles in a fluid medium, the ring being free to flow longitudinally. This system may be considered as a first approximation of a slurry system in laminar flow.

For the condition of turbulent flow it is expedient to base prediction equations for the head loss in a slurry on the results of experiments run under controlled conditions. As the first step it is desirable to reduce to a minimum the number of variables that must be investigated. This may be done by dimensional analysis. The form of the equation and the values of the constants may then be established from test data.

The phenomenon is assumed to involve the following variables:

<u>Symbol</u>	<u>Dimensions</u>	
ΔP	$ML^{-1}T^{-2}$	Pressure drop
L	L	Length of tube
D	L	Inside diameter of tube
r	-	Roughness of tube
ρ_f	ML^{-3}	Density of fluid
ρ_s	ML^{-3}	Density of solid particles
μ	$ML^{-1}T^{-1}$	Viscosity of fluid
d	L	Diameter of solid particles
e_s	-	Concentration of solids by weight
v_m	LT^{-1}	Velocity of mixture
g	LT^{-2}	Acceleration of gravity
α	-	Distribution factor

These 12 variables may be combined into 9 independent dimensionless groups to form the characteristic equation for the phenomenon. One form of the equation is

$$\frac{\Delta P}{\rho_f v_m^2} = \phi \left[\frac{L}{D}, r, \frac{\rho_f v_m D}{\mu}, \frac{\rho_s}{\rho_f}, e_s, \frac{d}{D}, \frac{v_m^2}{g D}, \alpha \right]. \quad (1)$$

If the fluid carries no solid particles the last five terms in equation (1) are not involved, and the equation reduces to

$$\frac{\Delta P}{\rho_f v_f^2} = \phi_1 \left[\frac{L}{D}, r, \frac{\rho_f v_f D}{\mu} \right]. \quad (2)$$

It is known that the variable, $\frac{L}{D}$, is separable when it is greater than approximately 20, so^D that

$$\frac{\Delta P}{\rho_f v_f^2} = \frac{L}{D} \phi_2 \left[r, \frac{\rho_f v_f D}{\mu} \right]. \quad (3)$$

The function ϕ_2 is usually replaced by a coefficient $\frac{f}{2}$, making it possible to rewrite equation (3) as

$$\frac{\Delta P}{\rho_f v_f^2} = \frac{f}{2} \frac{L}{D} \quad (4)$$

or

$$\Delta P = f \frac{L}{D} \frac{\rho_f v_f^2}{2}. \quad (5)$$

Equation (5) may also be written in terms of the head loss, H_f . Thus,

$$H_f = f \frac{L}{D} \frac{v_f^2}{2g}, \quad (6)$$

which is the familiar Darcy equation for head loss in a pipe. Charts have been developed for evaluating f for known values of the Reynolds number $\frac{\rho_f v_f D}{\mu}$ and the pipe roughness.

In extending the results to the flow of slurries it was assumed in this investigation that the quantity L/D in equation (1) was still separable, so that

$$\frac{\Delta P}{\rho_f v_m^2} = \frac{L}{D} \phi_3 \left[r, \frac{\rho_f v_m D}{\mu}, \frac{\rho_s}{\rho_f}, e_s, \frac{d}{D}, \frac{v_m^2}{g D}, \alpha \right]. \quad (7)$$

Since ϕ_2 in equation (3) is dependent on the turbulence of the fluid and since it was considered that the effect of solid particles in the slurry would be to alter the turbulence, it appeared reasonable to assume that ϕ_3 in equation (7) could be resolved into two component terms--one being the f of the fluid alone, the other being the solids coefficient which brings in the effect of the particles carried by the fluid. If this assumption is made, equation (7) becomes

$$\frac{\Delta P}{\rho_f v_m^2} = \frac{L}{D} \left[\frac{f}{2} + \frac{C_s}{2} \right] \quad (8)$$

or

$$H_f = (f + C_s) \frac{L}{D} \frac{v_m^2}{2g}, \quad (9)$$

in which C_s is the solids coefficient and f is the conventional Darcy coefficient based on the assumption that the conduit is carrying only fluid with a velocity v_m . Because of the complexity of the flow, particularly in the turbulent range, an analytical determination of C_s was not undertaken. Instead, it was evaluated from test data. The scope of the test program is indicated in Table II.

Table II

Material	Diameter (in.)	Concentration	Velocity (fps)
Glass	0.0012	7.7-10.0	2.0-14.9
	0.0020	9.4-27.5	2.0-16.6
	0.0026	0.4-34.8	0.5-17.2
	0.0114	0.9-48.5	0.1-18.3
	0.0314	3.8-59.6	0.4-19.3
Steel	0.0149	0.7-47.8	0.4-17.6
	0.0722	2.1-30.5	1.6-17.3
Lead	0.0505	3.1-63.8	1.4-17.9

From a comparison of equations (7) and (8) it appears reasonable to assume that C_s is a function of those variables in equation (7) that are not included in f .

$$C_s = \phi_4 \left[\frac{\rho_s}{\rho_f}, e_s, \frac{d}{D}, \frac{v_m^2}{g D}, \alpha \right]. \quad (10)$$

Since the three types of flow are directly related to α and can be identified readily, it is expedient to drop the α term from equation (10) and to develop a separate equation for each distribution.

Further consideration leads to the assumption that two of the principal effects of the particles are (1) to reduce turbulence by restricting the freedom of movement of the fluid and (2) to increase turbulence by interfering with straight-line flow of the fluid. These effects are geometrical, and may be described in terms of a geometrical factor--the relative portion of the tube cross-section occupied by solids, or the ratio A_S/A_T in which A_S denotes the effective area presented by the particles contained in a length d of the tube,* and A_T denotes the cross sectional area of the entire tube.

$$\frac{A_S}{A_T} = \frac{3}{2} \frac{e_s}{\left[\frac{\rho_s}{\rho_f} - e_s \left(\frac{\rho_s}{\rho_f} - 1 \right) \right]} \quad (11)$$

The variable e_s in equation (10) may be replaced by A_S/A_T , giving

$$C_s = \phi_5 \left[\frac{A_S}{A_T}, \frac{d}{D}, \frac{\rho_s}{\rho_f}, \frac{v_m^2}{g D} \right]. \quad (12)$$

Consideration of the data showed that the variables d/D and A_S/A_T were separable, and that the two remaining variables, ρ_f/ρ_s and $v_m^2/(g D)$ combined by multiplication. These findings permit equation (12) to be written in the form

$$C_s = \left(\frac{d}{D} \right)^n \frac{A_S}{A_T} \phi_6 \left[\frac{v_m^2}{g D} \frac{\rho_f}{\rho_s} \right] \quad (13)$$

or

$$\frac{C_s}{\left(\frac{d}{D} \right)^n \frac{A_S}{A_T}} = \phi_6 \left[\frac{v_m^2}{g D} \frac{\rho_f}{\rho_s} \right] \quad (14)$$

The dimensionless quantity, $\frac{v_m^2}{g D} \frac{\rho_f}{\rho_s}$, represents the ratio of the inertia force developed by a unit volume of the fluid to the gravitational force on a unit volume of the solid.

* This expression for A_S is derived in Appendix B.

RESULTS

The form of the expression for C_s in equation (14) was investigated by plotting values of the left hand side of equation (14) against values of the argument of ϕ_6 . The data gave linear plots on logarithmic coordinates as shown in Figs. 18 and 19 thus permitting n and ϕ_6 to be evaluated.

It will be observed that the exponent (n) was 0.20 for glass and -0.347 for the lead and steel, indicating a reversal in the effect of the diameter ratio on the solids coefficient. Figures 18 and 19 are plots of points that fell below the upper transition velocity (in the transition and low velocity regions). From Fig. 18 it can be seen that the two larger sizes of glass form one curve while the smaller diameter glass (0.0026 in. diam) forms a separate curve. The curve for sand was taken from a set of Miss Blatch's data (1). Since the curve for sand falls well above the curves for the glass particles, this tends to indicate that the shape and surface characteristics have a definite effect on the pressure drop.

In the higher velocity region, where the distribution is approximately constant, the pressure drop can be obtained from two relatively simple equations:

For glass,

$$\frac{\Delta P_m}{\Delta P_w} = 0.96 \left(\frac{D}{d} \right)^{0.076} \left(\frac{e}{s} \right)^{0.113} \quad (15)$$

For steel or lead,

$$\frac{\Delta P_m}{\Delta P_w} = 1.07 \quad (16)$$

where ΔP_w refers to water flowing at the same mean velocity as the suspension.

The results are summarized in Table III.

In the transition and low velocity regions a different pressure drop equation is indicated for the glass particles than for the lead or steel particles. The same situation appears to exist in the high velocity region. The effect of the diameter ratio is different in both cases. One possible explanation for this would be the existence of a critical size which is dependent upon the specific weight of the material. For particles below this critical size (glass particles in this investigation) the diameter ratio produced one effect while for particles above the critical size (lead and steel) an entirely different effect is indicated. At the present time insufficient data are available to prove or disprove this theory.

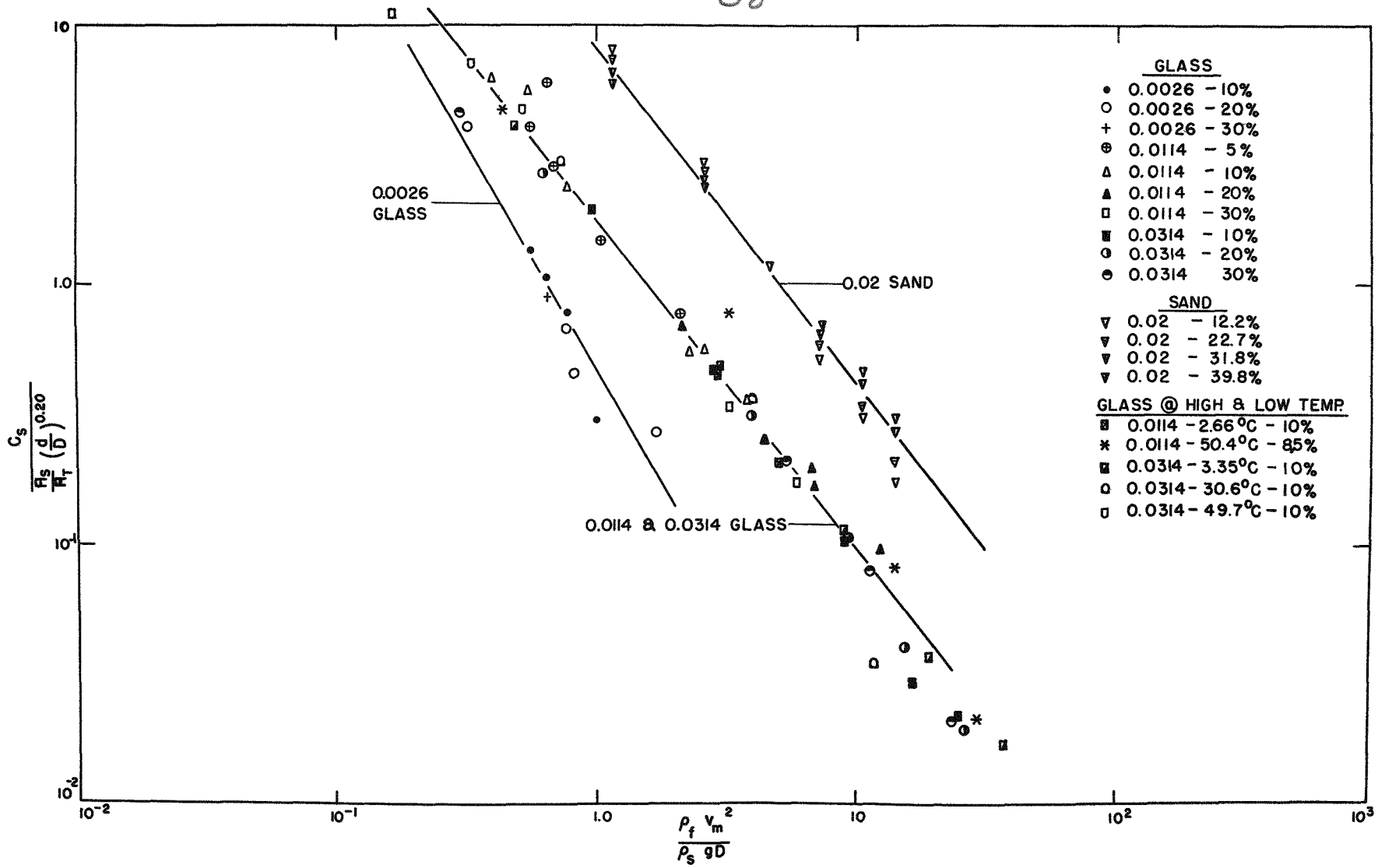


Fig. 18 - Solids coefficient for glass particles.

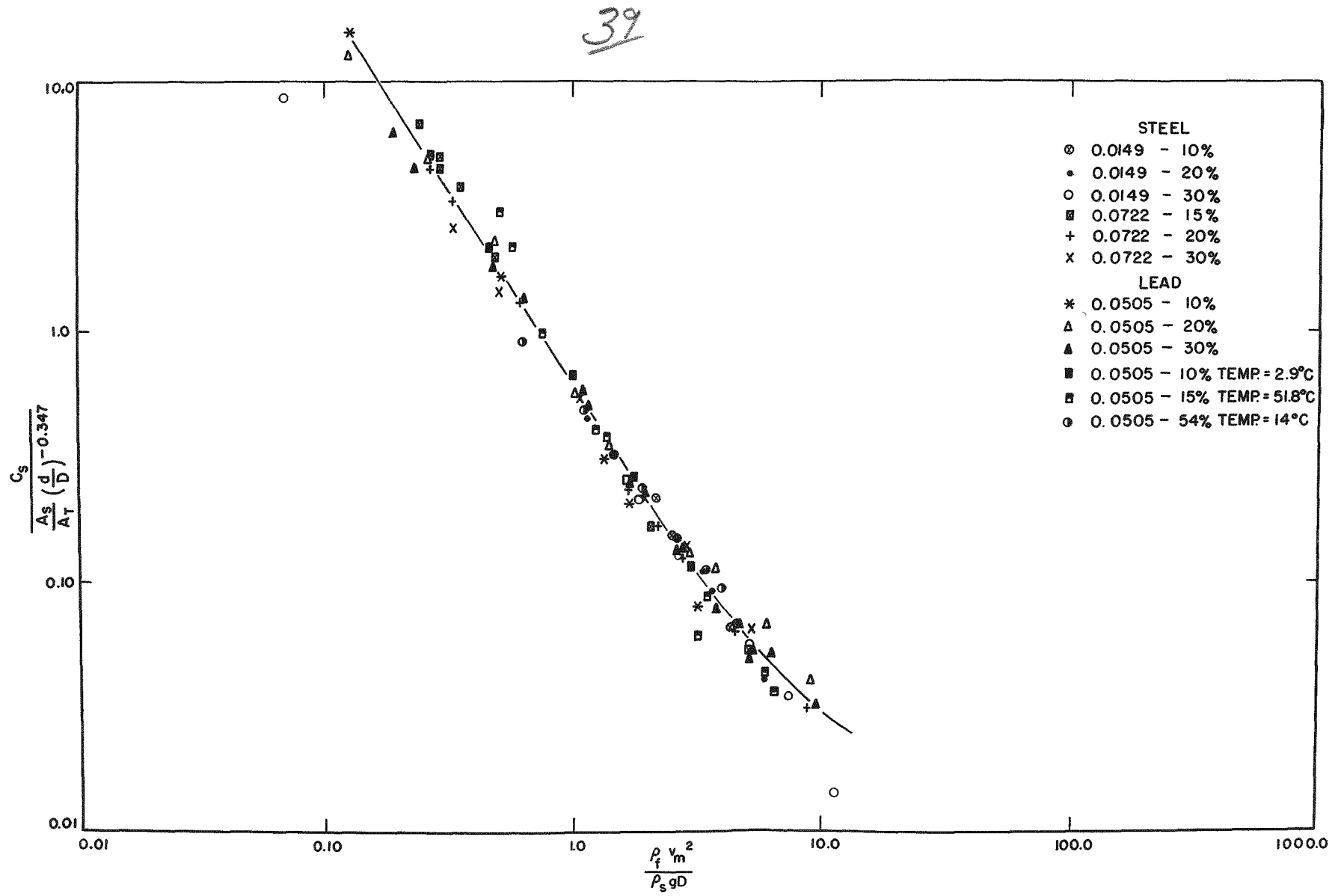


Fig. 19 - Solids coefficient for lead and steel particles.

Table III 40

Material	sp wt (pcf)	Size Range	Equations for Pressure Drop	
			Transition and low velocity region	High velocity region
Glass	146	0.004	No data obtained	$\frac{\Delta P_m}{\Delta P_w} = 0.96 \left(\frac{D}{d}\right)^{0.076} (e_s)^{0.113}$
	174	0.005	$\frac{\Delta P_m}{\rho_f v_m^2} = \frac{1}{2} \frac{L}{D} \sqrt{C_s + f}$ <p>C_s is obtained from Fig. 18</p>	
	178	0.023		
157	0.063			
Steel	465.0	0.030	$\frac{\Delta P_m}{\rho_f v_m^2} = \frac{1}{2} \frac{L}{D} \sqrt{C_s + f}$ <p>C_s is obtained from Fig. 19</p>	$\frac{\Delta P_m}{\Delta P_w} = 1.07$
	471.0	0.145		
Lead	705	0.102		

In order to predict the pressure drop it must be known what region of flow is being considered, high velocity, transition or low velocity. For the materials covered in this investigation the following equations give the approximate upper transition velocities. For lead and steel particles

$$\frac{\rho_f (v_{UT})^2}{\rho_s g D} = 75 \left(e_s \right)^{1.35} \quad (17)$$

For glass particles

$$\frac{\rho_f (v_{UT})^2}{\rho_s g D} = 285 \left[\frac{d}{D} e_s \right]^{0.6} \quad (18)$$

No explicit equation was found for the lower transition velocity, but Table IV gives the approximate range of values of v_{LT} for various concentrations and sizes. It will be noted that the

Table IV

Material	$\frac{\rho_f (v_{LT})^2}{\rho_s g D}$	Lower Transition velocity (fps)
Glass	0.9-0.4	1.9-1.2
Steel	1.6-0.6	4.0-2.5
Lead	1.5-0.5	4.8-2.9

viscosity of the fluid is not included as a variable in determining the solids coefficient (C_s) or the upper or lower transition velocities. In this investigation tests were run at both low and elevated temperatures (approximately 3 C to 50 C). These points are included in the data plotted on Figs. 18 and 19. From these it appears that the effect of viscosity on the pressure drop is taken care of by the term containing the conventional friction factor (f), and that ϕ_6 does not depend on the Reynolds number.

The effect of concentration may be shown by plotting the data on a different set of coordinate axes. If $\log \Delta p$ is plotted versus

log v for the same particles at different concentrations, curves similar to those shown in Fig. 20 are obtained. In the low velocity and transition regions that head loss increases with increasing concentration, but in the high velocity region, the reverse is true. It will be noted that the percentage difference in head loss is greater in the low velocity region than in the high velocity region. These effects of concentration were found for all mixtures investigated.

~~The mixer used was an Industrial Mixer (with a 1/30 hp motor, a 15 in. shaft, and a 3 in. propeller), which could be clamped onto the supply tank. This setup was used in obtaining the data for the 0.0020 in. diameter particles, ground glass and for part of the data for the 0.0026 in. diameter particles. In comparing the data taken by the original setup (using solids feed tank) with that taken using the mixer, no discrepancies were observed for the 0.0026 in. particles.~~

DESIGN CONSIDERATIONS

In the design of a system for pumping a fluid or suspension, it is important to determine the optimum conditions for minimum energy requirement. The conventional equation for horsepower (hp) is

$$hp = \frac{Q \Delta P}{550}, \quad (1)$$

where Q is the volume rate of flow (cfs), and ΔP is the pressure drop (psf). The rate of flow of the solid on a weight basis (q_s) (lb per sec) is

$$q_s = Q w_m e_s, \quad (2)$$

where w_m is the specific weight of the mixture (pcf) and e_s is the concentration of solid $\left[\frac{\text{lb of solid}}{\text{lb of mixture}} \right]$. If equation (2) is divided by (1) there results,

$$E = 550 \frac{w_m e_s}{\Delta P} \quad (3)$$

where E is the pounds of solid per second per horsepower and represents a transport effectiveness. Figure 21 is a typical plot of E versus velocity for different concentrations. These curves indicate that within the range investigated the maximum transport effectiveness is obtained at the lower transition velocity and at the maximum concentration of solid. For any velocity the transport effectiveness increases as the concentration increases.

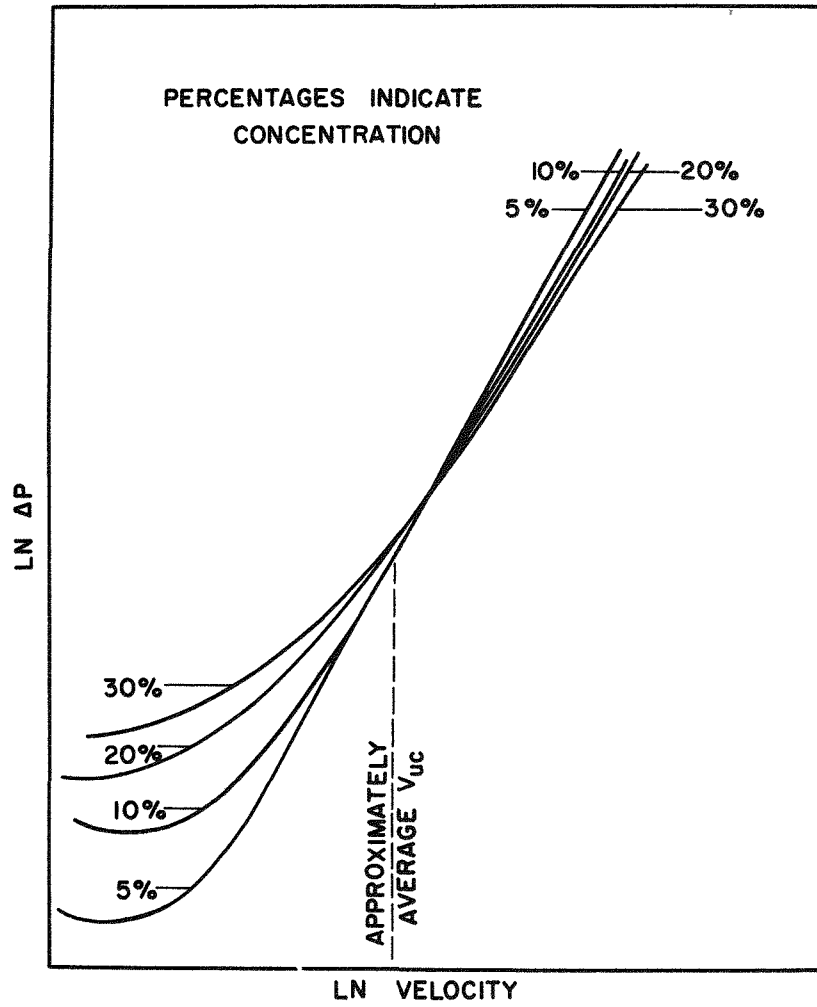


Fig. 20 - Typical pressure loss curves.

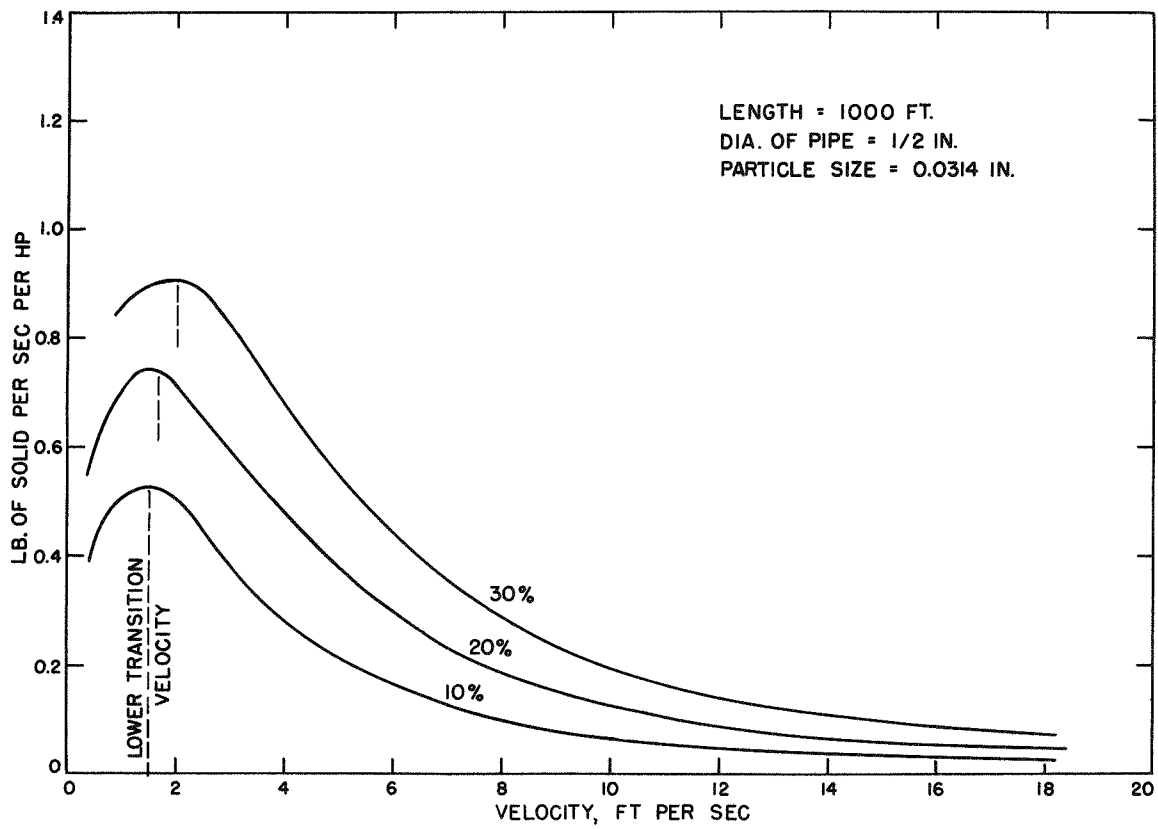


Fig. 21 - Transport effectiveness curves for 0.0314 in. glass particles.

The effect of particle size on the transport effectiveness is shown in Fig. 22. From the curves it can be seen that the maximum effectiveness is obtained at that lower transition velocity and the effectiveness at the velocity increases as the particle size decreases. However, at the higher velocities the larger particles give slightly higher values of E as is shown in Fig. 22(a). Figures 22 and 22(a) are for the glass particles which are all below the critical size. For particles above the critical size there is a reversal in the phenomenon as shown in Fig. 23. In the transition region the maximum E is obtained for the larger particles while in the high velocity region the difference between the values of E is negligible.

In some cases it may be desirable to have the solids uniformly distributed throughout the pipe. The minimum velocity at which this can be done corresponds approximately to the upper transition velocity. Values of E as a function of particle diameter are given in Fig. 24 for the two transition velocities and a velocity above the upper transition velocity. For pumping at the upper transition velocity the transport effectiveness increases as the size decreases for particles below the critical size.

The general conclusions indicated are for a size range of glass particles from a diameter of 0.0020 in. to 0.0314 in. What happens as the particle size varies outside of this range is not yet known and it is possible that an extrapolation of the results to other sizes might be misleading. As mentioned before, the critical size is believed to be a function of specific weight and therefore would have to be determined for each individual material.

CONCLUSIONS

Within the range of variables investigated the following conclusions appear to be valid.

I. General Flow Characteristics

1. There are three characteristic regions of flow:
(a) a high velocity region characterized by an approximately uniform distribution of solids throughout the tube; (b) a transition region characterized by a non-uniform distribution of solids, but with no stationary layer of particles; and (c) a low velocity region characterized by a stationary layer of particles.
2. The upper transition velocity, or boundary between the high velocity and the transition velocity regions, is a function of the particle size, and apparently there is a critical size for each material.

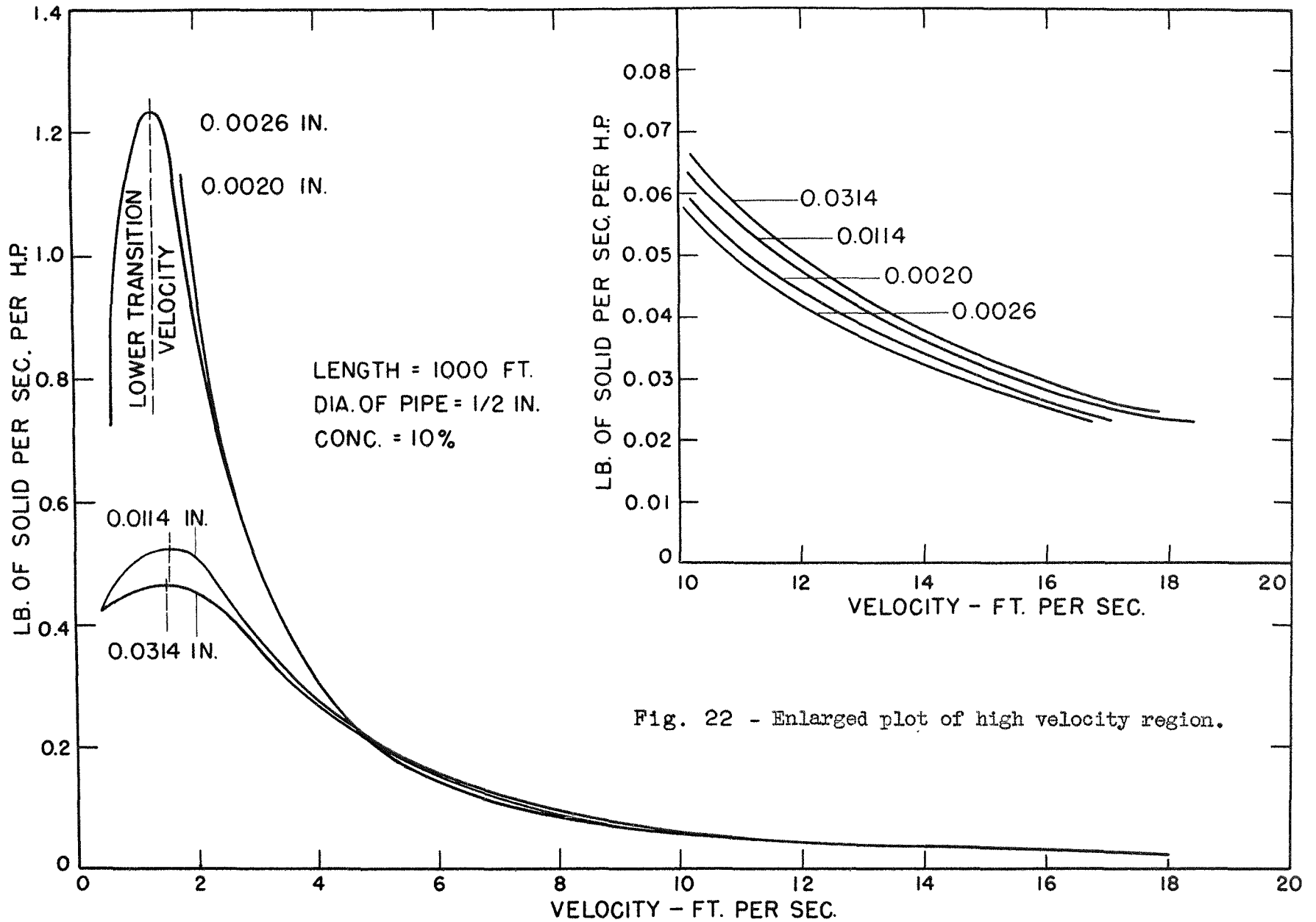


Fig. 22(a) - Transport effectiveness curves for glass particles.

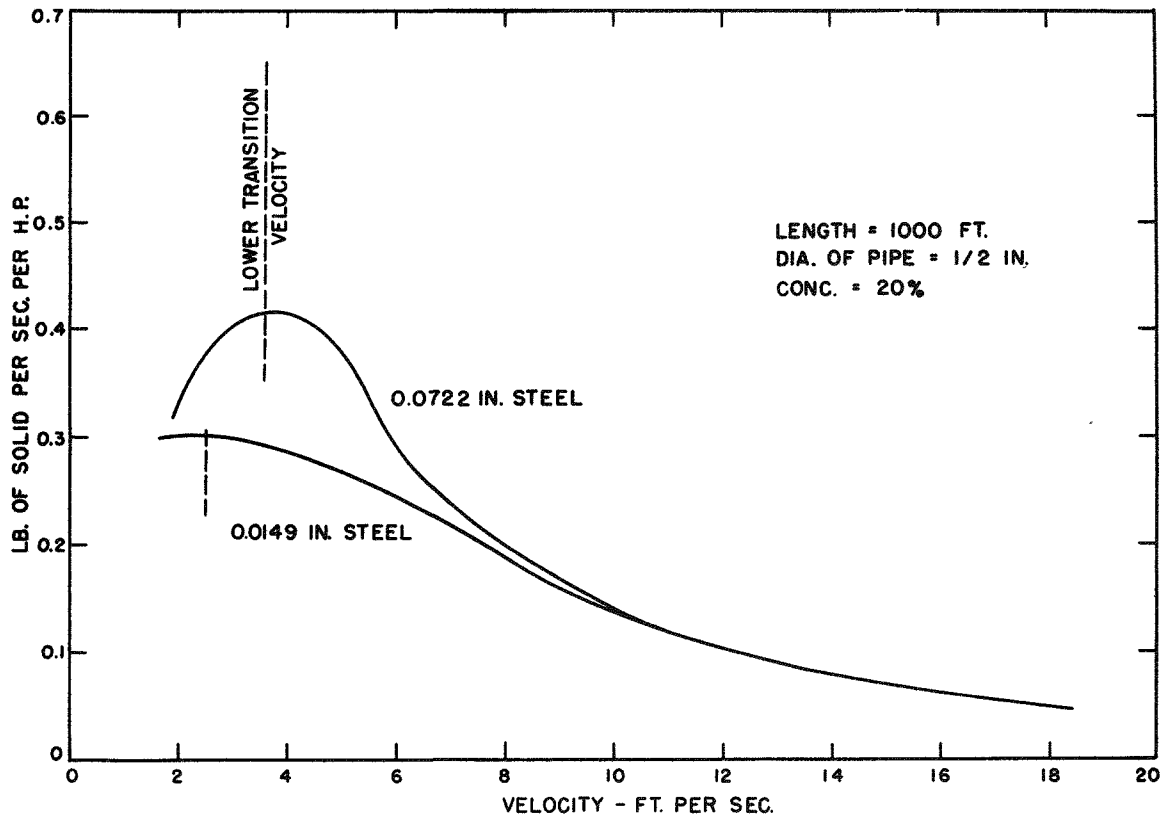


Fig. 23 - Transport effectiveness curves for steel particles.

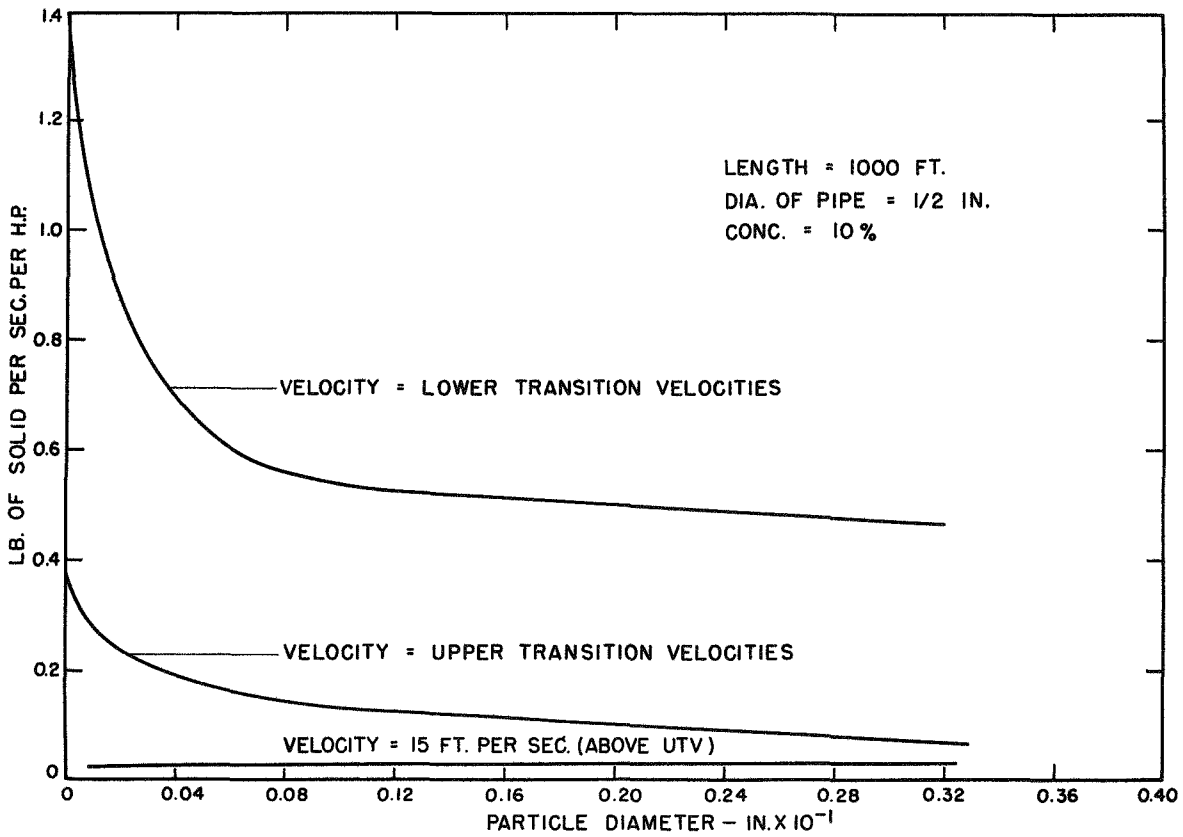


Fig. 24 - Transport effectiveness curves for glass particles.

3. For particles smaller than the critical size the upper transition velocity increases both as the concentration of solid and as the particle size increase. The following equation gives approximate values for the upper and transition velocities,

$$\frac{\rho_f (v_{UT})^2}{\rho_s g D} = 285 \left[\frac{d}{D} e_s \right]^{0.6}$$

4. For particles larger than the critical size the upper transition velocity increases as the concentration of solid increases. The following equation gives approximate values for the upper transition velocity,

$$\frac{\rho_f (v_{UT})^2}{\rho_s g D} = 75 e_s^{1.35}$$

5. The variation in the lower transition velocity is not sufficiently defined to indicate the variation with concentration and particle size.
6. Both the upper and lower transition velocities vary directly with the square root of the specific weight of the solid.

II. Pressure Drop Characteristics

1. The pressure drop in the transition and low velocity regions can be expressed by the equation,

$$\frac{\Delta P_m}{\rho_f v_m^2} = \frac{1}{2} \frac{L}{D} (C_s + f)$$

2. In the transition and low velocity regions:

- a. The pressure drop increases as the concentration increases.
- b. The pressure drop increases as the size increases for particles smaller than the critical size. The pressure drop decreases as the size increases for particles larger than the critical size.
- c. The magnitude of the solids coefficient (C_s) may be determined from a plot of

$$\frac{C_s}{\left[\frac{d}{D} \right]^n \frac{A_s}{A_T}} \quad \text{versus} \quad \frac{\rho_f v_m^2}{\rho_s g D}$$

3. In the high velocity region: a. For particles whose size is less than the critical size the pressure drop can be expressed as

$$\frac{\Delta P_m}{\Delta P_w} = 0.96 \left[\begin{array}{ccc} D & 0.076 & 0.113 \\ - & & \\ d & e_s & \end{array} \right]$$

For particles whose size is greater than the critical size the solids coefficient can be expressed as

$$\Delta P_m = 1.07 \Delta P_w .$$

4. The most economical velocity for pumping a slurry is the lower transition velocity.
5. The efficiency of pumping increases as the concentration of solid increases.

LITERATURE CITED

1. Babbitt, H. E. and Caldwell, D. H. Laminar flow of sludges in pipes with special reference to sewage sludge. Univ. of Ill. Eng. Exp. Sta. Bull. 319 (1939).
2. Babbitt, H. E. and Caldwell, D. H. Turbulent flow of sludges in pipes. Univ. of Ill. Eng. Exp. Sta. Bull. 323 (1940).
3. Blatch, N. S. Discussion: Water filtration at Washington, D. C. Trans. A.S.C.E. 57, 400-408 (1906).
4. Freudenthal, A. M. The inelastic behavior of engineering materials and structures. John Wiley and Sons, Inc., New York. 1950. First edition.
5. Howard, G. W. Transportation of sand and gravel in a four inch pipe. Proc. A.S.C.E. 64, 1377-1391 (1938).
6. Murphy, Glenn, Mitchell, W. I. and Young, D. F. Mechanical Characteristics of slurries. U. S. Atomic Energy Commission. ISC-237 (1952).
7. Murphy, Glenn, Mitchell, W. I. and Young, D. F. U. S. Atomic Energy Commission. ISC-236 (1952).
8. O'Brien, M. P. and Folsom, R. G. Transportation of sand in pipe lines. Univ. of Calif. Pub. in Eng. 3, 343-384 (1937).
9. Young, D. F. Flow of aqueous suspensions of rounded glass particles. Thesis (Unpublished), Iowa State College (1952).

ACKNOWLEDGMENTS

Warren I. Mitchell contributed many of the ideas incorporated in the original equipment and assisted materially in securing the data presented in the first part of the report.

Russell Crowther assisted with the analysis of the data.

APPENDIX A

Determination of Concentration

Concentration was defined as the ratio of the weight of the solid in a given volume of mixture to the weight of that volume of mixture. In all cases the concentration of the mixture was based on the mixtures as collected in a weighing tank after being pumped through the pressure drop system. It is recognized that the concentration of the mixture in a given length of pipe at any instant is different from the concentration of the mixture as collected because of "slip" between the particles and the liquid. However, the concentration as determined is the value of engineering significance from the standpoint of solids transportation.

The concentration may be expressed in terms of the specific weights of the solid, fluid, and mixture by utilizing the following basic relations

$$V_m = V_s + V_f \quad (1)$$

$$W_m = W_s + W_f \quad (1a)$$

$$\rho_s g = W_s/V_s \quad (1b)$$

$$\rho_f g = W_f/V_f \quad (1c)$$

$$\rho_m g = W_m/V_m \quad (1d)$$

By definition, the concentration is

$$e_s = \frac{W_s}{W_m} = \frac{W_s}{W_s + W_f} \quad (2)$$

$$e_s = \frac{\rho_s V_s}{\rho_s V_s + \rho_f V_f} \quad (3)$$

The reciprocal of equation (3) gives

$$\frac{1}{e_s} = 1 + \frac{\rho_f}{\rho_s} \left(\frac{V_f}{V_s} \right) \quad (4)$$

$$\frac{1}{e_s} = 1 + \frac{\rho_f}{\rho_s} \left(\frac{V_m - V_s}{V_s} \right) \quad (5)$$

$$\frac{1}{e_s} = 1 + \frac{\rho_f}{\rho_s} \left(\frac{V_m}{V_s} - 1 \right) \quad (5a)$$

By replacing the volumes in equation (5a) by equations (1b) and (1d) the form

$$\begin{aligned} \frac{1}{e_s} &= 1 + \frac{\rho_f}{\rho_s} \left[\frac{\frac{W_m}{\rho_m}}{\frac{W_s}{\rho_s}} - 1 \right] \\ &= 1 + \frac{\rho_f}{\rho_s} \left[\frac{W_m \rho_s}{W_s \rho_m} - 1 \right] \end{aligned} \quad (6)$$

is obtained.

Then from the definition of concentration, equation (2), equation (6) becomes

$$\frac{1}{e_s} = 1 + \frac{\rho_f}{\rho_s} \left[\frac{1}{e_s} \frac{\rho_s}{\rho_m} - 1 \right], \quad (7)$$

from which is obtained

$$e_s = \frac{\frac{\rho_s}{\rho_f} - \frac{\rho_s}{\rho_m}}{\frac{\rho_s}{\rho_f} - 1} \quad (8)$$

Sample curves are shown in Figs. A1, A2, and A3 of concentration versus specific weight of the mixture for the particles of various specific weights used in this investigation.

APPENDIX B

Determination of Projected Area of Particles

It was desired to obtain an expression for the area projected by the solids on a cross section of the tube. To obtain this expression several assumptions were made.

The first assumption was that the particles were all the same diameter and were perfect spheres. The second assumption was that the particles were enclosed in small imaginary discs whose diameter was the diameter of the tube and whose thickness was the diameter of the particles enclosed in it (see Fig. B1), and that these discs moved through the tube without any particles entering or leaving each individual disc. The third assumption was that the total projected area was the area projected by the particles in any one disc and that the particles in the disc directly behind could not be "seen." Lastly, it was assumed that the weight of solid in the disc was the concentration times the weight of the disc.

The weight of the solid per disc was first established as

$$W_s = e_s W_m = e_s V_m \rho_m g = e_s V_T \rho_m g \quad (1)$$

An expression was then written for the number of particles per disc

$$N = \frac{W_s}{W_p} = \frac{e_s V_T \rho_m g}{\frac{\pi d^3 \rho_s g}{6}} = 6 \frac{e_s V_T \rho_m}{\pi d^3 \rho_s} \quad (2)$$

The total projected area of the solids was

$$A_s = N A_p = 6 \left[\frac{e_s V_T \rho_m}{\pi d^3 \rho_s} \right] \left[\frac{\pi d^2}{4} \right] \quad (3)$$

$$A_s = \frac{1.5 e_s V_T \rho_m}{d \rho_s}$$

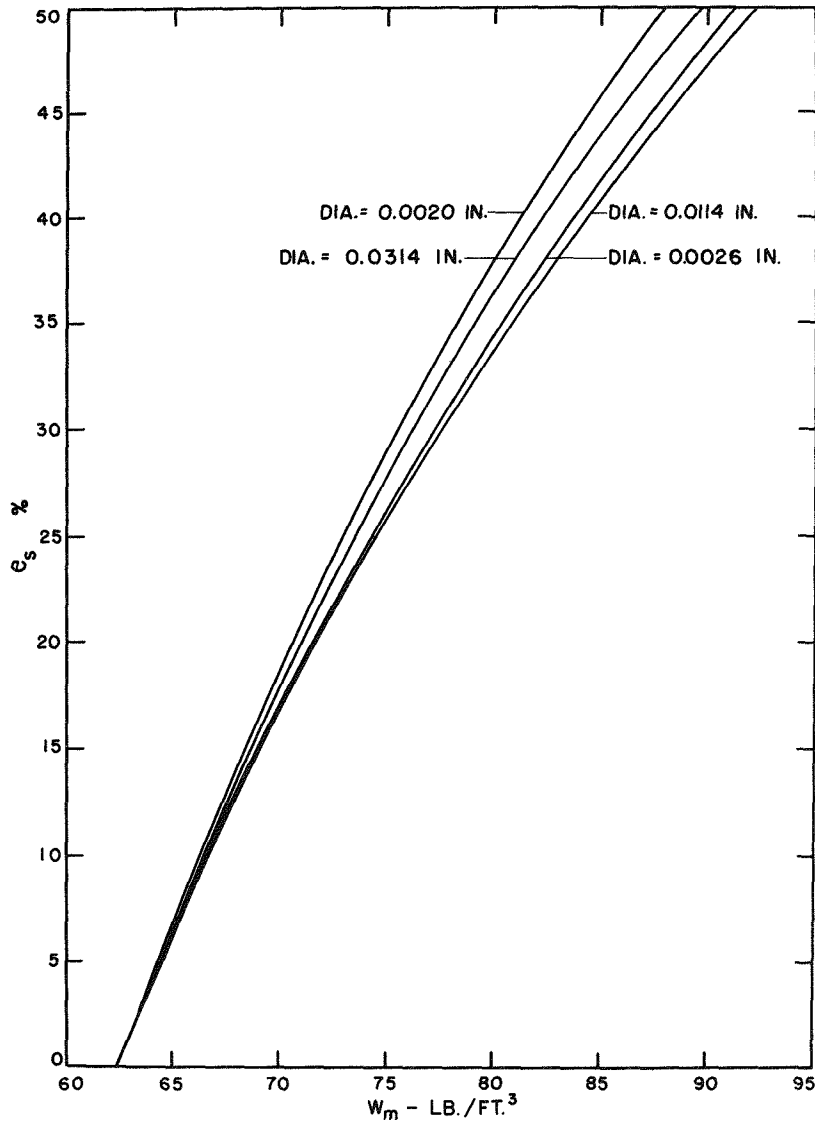


Fig. A1 - Relation between concentration and specific weight for glass.

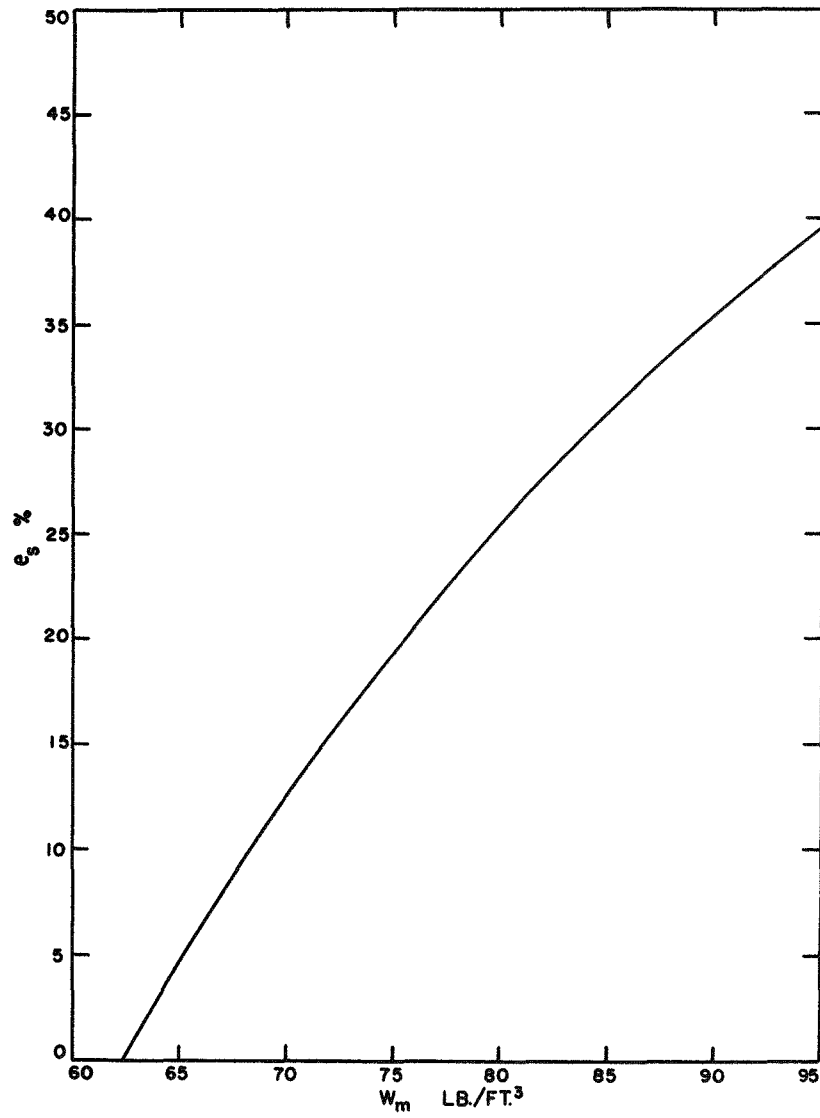


Fig. A2 - Relation between concentration and specific weight for steel.

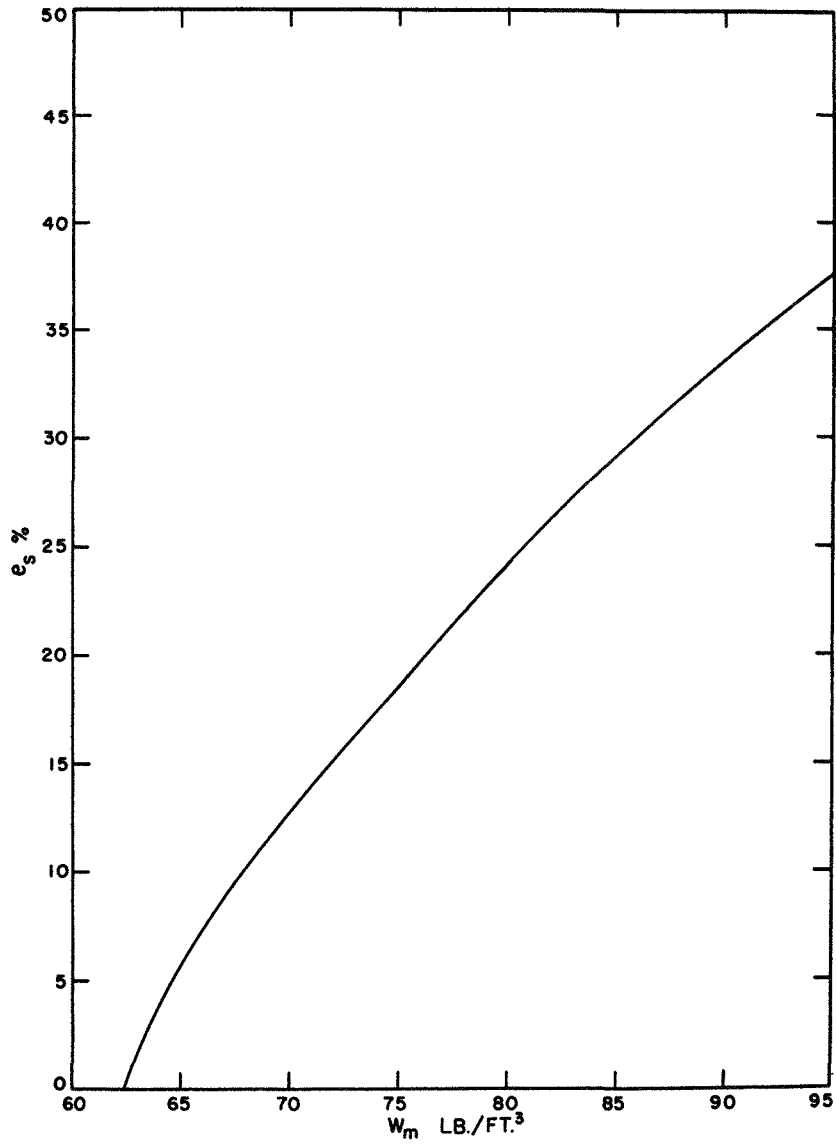


Fig. A3 - Relation between concentration and specific weight for lead.

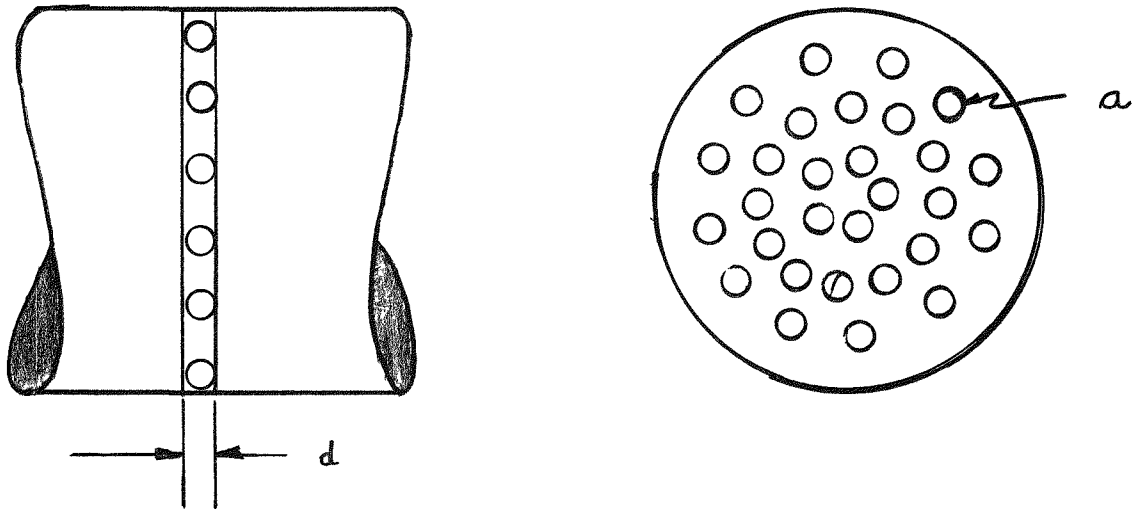


Fig. B1 - Effective area of solid A_s .

Replacing the volume by its equivalent gave

$$\begin{aligned}
 A_s &= \frac{1.5 e_s \rho_m}{d \rho_s} \left[\frac{\pi D^2}{4} d \right] & (3a) \\
 &= \frac{3}{8} \frac{e_s \pi D^2 \rho_m}{\rho_s}
 \end{aligned}$$

Substituting in equation (3a) a form of the equation previously derived for concentration gave the final equation for the total projected area.

$$A_s = \frac{3}{8} \frac{e_s \pi D^2}{\frac{\rho_s}{\rho_f} - e_s \left[\frac{\rho_s}{\rho_f} - 1 \right]} \quad (4)$$

APPENDIX C

Table I

Material: Glass
 Diameter of Particle: 0.00122 in.
 Specific Weight: 146.2 pcf

Reference Number	Temperature (°C)	Concentration (%)	Mean velocity of mixture (fps)	Head loss (ft of mixture/ft)
1	22.0	9.6	2.01	0.0475
2	20.0	7.8	3.57	0.139
3	19.0	9.6	7.12	0.506
4	19.0	5.4	9.99	0.890
5	17.4	10.1	12.80	1.39
6	18.2	10.0	14.94	1.87

Table II

Material: Glass
 Diameter of Particle: 0.0020 in.
 Specific Weight: 146.2 pcf

Reference Number	Temperature (°C)	Concentration (%)	Mean velocity of mixture (fps)	Head loss (ft of mixture/ft)
1	24.4	9.5	1.98	0.0530
2	20.0	10.3	7.68	0.585
3	19.0	9.7	10.62	1.01
4	19.0	9.4	13.42	1.50
5	19.0	9.7	16.63	2.24
6	23.6	18.4	1.99	0.0512
7	18.5	17.0	4.66	0.238
8	21.4	17.7	7.49	0.538
9	19.5	18.1	10.13	0.929
10	18.3	20.3	12.77	1.41
11	18.2	18.0	16.01	2.09
12	20.0	25.9	7.27	0.538
13	16.8	26.2	11.32	1.16
14	14.8	27.5	15.55	2.03

Table III

Material: Glass
 Diameter of Particle: 0.0026 in.
 Specific Weight: 174.0 pcf

Reference Number	Temperature (°C)	Concentration (%)	Mean velocity of mixture (fps)	Head loss (ft. of mixture/ft)
1	16.0	0.4	0.900	0.0527
2	14.6	0.4	1.47	0.0394
3	14.1	0.9	1.87	0.0459
4	13.8	1.4	4.02	0.183
5	13.9	0.4	5.41	0.300
6	14.0	0.4	7.40	0.532
7	13.0	0.4	9.35	0.804
8	14.0	0.8	9.40	0.825
9	14.0	0.4	9.50	0.681
10	16.7	1.6	13.82	1.58
11	16.5	2.0	17.20	2.32
12	16.2	3.2	1.06	0.0480
13	14.8	4.7	1.67	0.0478
14	15.0	3.6	2.58	0.0861
15	16.2	7.0	3.72	0.163
16	15.1	3.3	3.82	0.167
17	15.0	4.6	5.17	0.284
18	15.3	4.6	6.67	0.449
19	16.6	4.5	7.75	0.590
20	14.0	4.3	8.40	0.663
21	13.2	3.7	9.50	0.830
22	17.2	4.3	11.90	1.24
23	17.2	4.6	14.62	1.80
24	17.0	5.0	16.80	2.29
25	17.3	8.8	0.655	0.0754
26	17.0	8.5	1.43	0.0467
27	14.0	8.1	1.54	0.0478
28	14.1	11.3	1.68	0.0504
29	14.3	9.3	1.92	0.0517
30	13.9	9.7	3.77	0.169
31	18.0	10.9	6.83	0.462
32	21.0	10.9	6.96	0.478
33	15.9	9.7	8.15	0.642
34	16.6	9.6	9.60	0.846
35	17.6	11.2	10.03	0.955
36	17.9	11.1	13.27	1.57
37	17.6	11.1	16.38	2.26

Table III (Continued)

Reference Number	Temperature (°C)	Concentration (%)	Mean velocity of mixture (fps)	Head loss (ft of mixture/ft)
38	15.3	15.5	0.731	0.0718
39	14.5	14.8	1.45	0.0574
40	14.5	14.8	1.64	0.0530
41	14.0	17.0	2.11	0.0647
42	13.8	13.2	2.60	0.0908
43	17.5	13.2	5.25	0.303
44	13.7	16.2	6.65	0.462
45	15.8	15.1	6.79	0.483
46	14.0	16.0	8.20	0.660
47	13.9	13.5	8.30	0.681
48	14.0	15.2	9.27	0.820
49	17.7	14.7	10.77	1.07
50	19.0	14.4	12.80	1.43
51	18.3	14.1	16.00	2.17
52	15.8	18.2	1.08	0.0736
53	14.8	20.8	1.67	0.0564
54	14.8	19.6	1.73	0.0509
55	14.0	19.0	2.50	0.0851
56	14.8	19.9	5.33	0.303
57	14.8	18.1	8.86	0.760
58	13.0	19.0	9.80	0.710
59	18.3	18.1	9.95	0.924
60	20.0	18.9	12.49	1.37
61	19.8	18.9	15.73	2.08
62	16.0	25.3	1.01	0.0825
63	15.8	24.9	1.03	0.0749
64	15.8	24.5	1.65	0.0621
65	15.8	24.0	1.67	0.0525
66	13.8	26.5	1.68	0.0598
67	14.9	22.6	1.85	0.0538
68	15.7	24.5	2.00	0.0600
69	14.2	27.2	2.23	0.0702
70	14.0	24.6	4.97	0.279
71	18.0	26.9	9.11	0.788
72	16.6	28.8	0.494	0.0138
73	14.3	28.4	1.54	0.0710
74	15.9	28.1	2.13	0.0655
75	15.3	27.7	2.14	0.0647
76	15.2	29.2	8.65	0.713
77	20.0	29.4	14.90	1.89

Table III (Continued)

Reference Number	Temperature (°C)	Concentration (%)	Mean velocity of mixture (fps)	Head loss (ft. of mixture/ft)
78	14.9	34.3	1.21	0.0820
79	17.2	33.3	1.77	0.0512
80	16.3	32.9	6.64	0.452
81	18.0	34.8	9.50	0.827

Table IV

Material: Glass
 Diameter of Particle: 0.0114 in.
 Specific Weight: 177.8 pcf

Reference No.	Temperature (°C)	Concentration (%)	Mean velocity of mixture (fps)	Head loss (ft of mixture)/ft
1	9.0	7.3	0.433	0.162
2	3.2	9.5	1.54	0.125
3	3.8	9.5	2.31	0.134
4	3.0	9.0	4.80	0.295
5	5.2	7.7	6.62	0.488
6	2.2	9.2	8.75	0.791
7	9.0	7.7	8.95	0.770
8	7.0	19.7	0.52	0.216
9	5.1	18.8	1.61	0.172
10	3.8	21.8	3.28	0.206
11	2.8	18.8	4.34	0.258
12	2.2	17.1	6.12	0.470
13	3.0	21.5	6.14	0.446
14	1.5	19.9	8.34	0.752
15	8.0	28.1	0.489	0.244
16	3.3	28.9	1.58	0.202
17	2.7	29.5	3.08	0.212
18	3.2	30.8	5.46	0.358
19	3.0	30.0	6.70	0.499
20	5.6	37.4	1.77	0.244
21	21.0	0.9	1.69	0.0611
22	13.5	0.7	2.90	0.102
23	12.5	1.1	5.23	0.284
24	12.5	1.1	6.91	0.457
25	12.3	1.1	8.37	0.642
26	12.3	0.6	9.14	0.744
27	12.9	2.3	9.34	0.741
28	20.0	5.0	0.530	0.0927
29	14.3	3.9	1.44	0.0663
30	14.7	6.8	1.56	0.0994
31	15.2	5.0	1.61	0.0679
32	14.8	5.0	1.96	0.0739
33	15.8	5.9	2.82	0.118
34	14.0	3.1	3.83	0.179
35	13.5	7.1	5.05	0.298

Table IV (Continued)

Reference No.	Temperature (°C)	Concentration (%)	Mean velocity of mixture (fps)	Head loss (ft of mixture)/ft
36	13.0	4.2	5.21	0.305
37	17.8	3.2	5.32	0.290
38	15.3	4.8	6.86	0.465
39	14.0	4.0	8.35	0.647
40	14.0	4.6	9.11	0.749
41	13.0	4.9	9.66	0.835
42	14.5	5.5	9.94	0.833
43	14.3	4.5	9.97	0.851
44	12.5	3.0	10.32	0.916
45	12.7	4.9	10.78	0.992
46	12.9	5.7	10.82	0.981
47	16.2	6.7	15.87	1.89
48	15.5	3.7	18.10	2.40
49	18.0	9.7	0.460	0.134
50	16.5	10.0	1.22	0.104
51	16.8	10.5	1.43	0.131
52	21.0	8.1	1.69	0.0981
53	14.8	8.5	2.90	0.133
54	14.5	7.8	3.11	0.153
55	14.0	8.5	3.77	0.188
56	13.2	9.8	5.07	0.290
57	19.7	10.5	7.01	0.472
58	16.6	9.1	9.06	0.752
59	17.5	9.8	9.55	0.778
60	16.0	9.8	10.03	0.861
61	17.1	8.1	12.90	1.31
62	16.1	9.4	17.90	2.31
63	15.5	9.1	18.30	2.35
64	17.5	13.2	0.540	0.159
65	21.5	17.3	0.932	0.146
66	14.7	15.6	1.12	0.126
67	16.0	13.2	2.13	0.137
68	15.8	15.2	2.14	0.137
69	19.8	13.2	2.47	0.132
70	14.3	13.4	3.60	0.183
71	13.5	14.1	5.11	0.305
72	13.3	14.9	8.08	0.634
73	13.4	16.6	8.38	0.671
74	20.5	13.5	8.51	0.642
75	13.7	13.9	9.23	0.780
76	13.0	12.7	9.48	0.804
77	15.1	15.9	9.76	0.856
78	16.5	15.2	13.90	1.45
79	13.7	15.0	15.37	1.74
80	15.8	15.2	18.10	2.28

Table IV (Continued)

Reference No.	Temperature (°C)	Concentration (%)	Mean velocity of mixture (fps)	Head loss (ft. of mixture)/ft
81	19.5	18.3	0.440	0.193
82	14.5	22.0	2.82	0.181
83	14.7	19.5	4.09	0.231
84	13.5	19.9	5.05	0.313
85	14.0	19.1	5.10	0.305
86	14.7	17.8	6.84	0.457
87	17.0	21.6	7.83	0.569
88	13.3	18.6	9.35	0.796
89	16.0	20.5	17.11	2.01
90	15.5	19.7	17.93	2.22
91	16.1	18.8	18.10	2.27
92	19.3	23.7	0.410	0.181
93	16.0	24.2	1.57	0.178
94	14.0	26.9	4.52	0.298
95	17.0	27.0	5.20	0.311
96	15.0	26.0	6.86	0.475
97	13.3	26.9	8.20	0.637
98	16.0	23.5	9.32	0.765
99	17.0	23.5	14.30	1.48
100	16.5	25.8	17.90	2.17
101	15.7	27.8	0.790	0.200
102	18.0	27.7	3.46	0.217
103	13.8	30.0	4.71	0.290
104	14.0	32.2	9.91	0.835
105	13.4	29.3	10.19	0.861
106	14.8	30.4	18.17	2.20
107	17.0	36.5	2.42	0.231
108	14.0	35.6	4.32	0.298
109	15.5	34.2	6.80	0.465
110	21.0	40.9	0.360	0.251
111	18.2	40.8	1.14	0.237
112	16.3	38.8	1.32	0.218
113	16.0	39.1	1.77	0.221
114	15.3	39.0	9.73	0.762
115	16.3	48.3	2.40	0.292
116	17.0	43.5	6.16	0.392
117	21.0	48.5	6.39	0.425

Table IV (Continued)

Reference No.	Temperature (°C)	Concentration of mixture (%)	Mean velocity of mixture (fps)	Head loss (ft of mixture)/ft
118	31.7	7.7	0.348	0.139
119	30.2	8.2	1.74	0.109
120	30.0	10.1	3.40	0.164
121	29.8	10.1	5.89	0.331
122	29.8	12.5	7.30	0.470
123	29.8	10.2	8.98	0.652
124	33.1	18.0	0.388	0.184
125	31.3	18.7	1.37	0.152
126	30.4	19.9	3.38	0.190
127	30.3	18.9	5.78	0.329
128	30.0	18.9	7.47	0.488
129	30.0	20.5	8.96	0.642
130	32.3	27.3	0.521	0.214
131	30.8	30.2	1.27	0.188
132	30.0	30.2	3.74	0.234
133	30.2	30.0	6.20	0.365
134	30.2	28.8	7.98	0.522
135	30.2	27.8	9.05	0.637
136	51.3	9.0	0.323	0.103
137	51.0	7.8	0.505	0.102
138	50.0	7.8	1.28	0.0783
139	50.0	9.5	3.48	0.173
140	50.0	7.9	7.30	0.415
141	50.0	8.9	10.50	0.749
142	49.0	18.9	0.275	0.195
143	50.7	17.9	0.322	0.185
144	48.2	18.5	0.860	0.145
145	50.5	19.8	1.26	0.144
146	49.2	22.5	2.11	0.193
147	49.5	19.7	5.72	0.300
148	50.0	18.4	8.16	0.496
149	49.2	20.6	10.30	0.710
150	47.0	30.6	0.141	0.194
151	49.2	30.2	0.405	0.222
152	49.3	29.6	1.75	0.177
153	48.0	28.2	2.94	0.206
154	48.1	28.5	5.76	0.326
155	48.0	33.0	9.89	0.642

Table V

Material: Glass
 Diameter of Particle: 0.0314 in.
 Specific Weight: 156.2 pcf

Reference No.	Temperature (°C)	Concentration (%)	Mean velocity of mixtures (fps)	Head loss (ft of mixture)/ft
1	4.2	10.7	0.759	0.158
2	4.3	9.8	1.29	0.113
3	1.9	10.0	3.13	0.173
4	3.7	8.1	5.48	0.347
5	4.5	9.0	7.98	0.606
6	4.0	9.9	11.20	1.07
7	3.7	7.6	13.00	1.56
8	1.5	9.7	17.10	2.30
9	15.2	5.1	1.00	0.104
10	14.8	6.0	1.35	0.0903
11	14.0	4.7	3.08	0.146
12	13.7	3.8	5.79	0.331
13	13.2	6.2	7.09	0.477
14	13.5	6.3	9.02	0.697
15	16.0	5.4	13.30	1.44
16	14.8	5.4	15.59	1.80
17	15.0	6.7	17.10	2.12
18	16.5	4.1	17.68	2.27
19	15.7	6.0	18.50	2.39
20	16.9	10.1	0.601	0.126
21	14.5	9.8	1.78	0.118
22	13.8	9.0	3.04	0.155
23	13.7	10.8	5.46	0.313
24	14.0	10.8	7.44	0.488
25	13.9	12.4	9.14	0.697
26	15.0	8.8	11.90	1.10
27	17.2	8.8	13.59	1.37
28	14.7	9.8	15.60	1.78
29	15.5	10.0	17.79	2.01
30	18.0	15.7	0.352	0.145
31	15.8	17.0	1.25	0.126
32	16.0	17.3	2.98	0.192
33	14.0	17.2	5.75	0.352
34	14.0	15.8	7.36	0.491
35	14.0	17.0	9.20	0.684
36	14.7	15.8	14.59	1.52
37	15.7	15.0	18.20	2.21

Table V (Continued)

Reference No.	Temperature (°C)	Concentration (%)	Mean velocity of mixture (fps)	Head loss (ft. of mixture)/ft
38	19.5	18.8	0.442	0.158
39	15.0	18.8	1.44	0.170
40	14.0	19.9	3.62	0.229
41	14.0	21.8	5.55	0.347
42	15.0	19.2	7.13	0.459
43	14.0	21.8	9.33	0.697
44	15.0	21.5	14.78	1.49
45	14.8	18.0	17.55	2.04
46	17.3	19.0	18.50	2.14
47	17.0	25.2	0.845	0.174
48	14.7	27.0	14.65	1.41
49	14.5	26.0	16.00	1.67
50	16.9	32.5	0.995	0.189
51	16.8	33.2	1.45	0.195
52	16.0	29.5	4.21	0.295
53	15.5	32.0	6.15	0.410
54	15.5	32.9	8.24	0.566
55	14.0	30.3	8.90	0.624
56	14.7	30.5	15.10	1.47
57	14.8	29.5	15.53	1.57
58	14.8	32.4	18.68	2.03
59	16.0	46.6	1.37	0.251
60	18.5	50.2	1.67	0.258
61	17.0	45.8	5.30	0.394
62	14.0	46.8	8.11	0.579
63	14.5	45.1	9.08	0.660
64	16.0	59.6	3.50	0.352
65	14.0	55.1	5.79	0.501
66	14.0	52.3	7.06	0.532
67	29.4	6.6	18.47	2.23
68	31.5	9.2	0.652	0.126
69	32.0	11.0	1.54	0.119
70	30.2	10.2	3.59	0.179
71	30.0	10.2	6.25	0.334
72	30.2	10.0	8.35	0.532
73	30.8	9.2	12.57	1.10
74	30.5	9.7	14.86	1.49
75	29.2	10.3	18.49	2.19

Table V (Continued)

Reference No.	Temperature (°C)	Concentration (%)	Mean velocity of mixture (fps)	Head loss (ft. of mixture)/ft
76	49.5	6.3	3.54	0.147
77	49.0	9.2	1.05	0.114
78	49.0	9.2	1.31	0.105
79	48.5	9.2	3.64	0.155
80	49.0	12.3	6.15	0.308
81	50.0	11.3	9.43	0.590
82	50.7	11.3	13.03	1.06
83	50.0	11.0	15.50	1.46
84	51.2	10.3	19.28	2.16
85	46.0	13.2	0.605	0.129
86	48.2	13.7	1.37	0.122

Table VI

Material: Steel
 Diameter of Particle: 0.0149 in.
 Specific Weight: 468 pcf

Reference No.	Temperature (°C)	Concentration (%)	Mean velocity of mixture (fps)	Head loss (ft. of mixture)/ft
1	13.5	1.8	5.28	0.287
2	12.4	0.7	7.00	0.467
3	13.3	1.5	8.14	0.600
4	12.3	1.7	8.35	0.632
5	13.8	2.1	8.94	0.699
6	12.3	0.7	9.65	0.809
7	17.2	5.7	0.560	0.199
8	14.2	4.6	1.87	0.177
9	13.5	3.0	2.83	0.118
10	13.3	4.6	3.00	0.185
11	13.3	4.0	3.62	0.178
12	13.3	5.9	3.91	0.218
13	12.8	5.1	4.37	0.232
14	12.5	3.3	5.15	0.282
15	12.5	3.2	6.00	0.371
16	12.3	5.0	6.95	0.467
17	14.0	7.2	8.35	0.619
18	14.2	6.3	8.43	0.626
19	14.3	5.9	9.60	0.780
20	15.0	4.1	9.68	0.791
21	14.9	6.2	12.63	1.23
22	14.8	6.4	17.58	2.18
23	14.2	11.7	4.64	0.321
24	13.7	11.6	4.91	0.313
25	14.2	11.7	6.54	0.436
26	12.4	10.2	6.72	0.462
27	13.8	9.5	9.48	0.752
28	14.8	11.7	12.80	1.20
29	16.5	12.1	17.30	2.05
30	19.8	13.2	0.354	0.311
31	18.5	13.9	0.463	0.277
32	16.2	13.2	1.19	0.316
33	16.0	12.5	1.55	0.236
34	14.3	14.5	2.24	0.331
35	14.2	14.6	2.73	0.308
36	13.8	12.8	3.95	0.284
37	12.7	16.1	7.85	0.585

Table VI (Continued)

Reference No.	Temperature (°C)	Concentration (%)	Mean velocity of mixture (fps)	Head loss (ft. of mixture)/ft
38	13.8	14.7	9.37	0.731
39	13.0	17.3	9.51	0.744
40	13.5	13.1	11.80	0.767
41	15.5	13.3	12.70	1.19
42	15.3	14.4	17.56	2.07
43	16.3	22.3	1.35	0.384
44	14.5	21.9	3.38	0.371
45	13.7	21.6	5.76	0.454
46	14.0	21.5	6.05	0.459
47	13.8	18.7	7.74	0.566
48	14.6	18.2	9.47	0.707
49	15.5	18.1	13.08	1.18
50	16.7	20.6	17.62	1.97
51	14.8	23.0	1.48	0.428
52	14.2	25.5	2.19	0.418
53	14.0	26.2	2.62	0.360
54	12.7	25.6	5.50	0.449
55	13.8	25.0	7.29	0.561
56	13.3	25.0	7.36	0.579
57	13.3	25.5	9.16	0.699
58	15.5	23.0	13.24	1.17
59	16.2	24.7	17.63	1.87
60	32.1	27.6	0.836	0.407
61	14.0	29.4	4.29	0.436
62	14.0	32.0	5.16	0.449
63	12.7	29.5	7.17	0.564
64	12.7	27.6	8.60	0.671
65	16.2	28.2	10.56	0.804
66	15.6	31.4	13.48	1.12
67	16.5	29.7	17.62	1.79
68	15.8	36.6	13.78	1.10
69	12.0	41.8	0.913	0.514
70	14.5	47.8	2.54	0.488
71	14.8	40.8	6.30	0.514

Table VII

Material: Steel
 Diameter of Particle: 0.0722 in.
 Specific Weight: 468 pcf

Reference No.	Temperature (°C)	Concentration (%)	Mean velocity of mixture (fps)	Head loss (ft. of mixture)/ft
1	14.1	2.1	9.85	0.801
2	14.1	7.5	3.36	0.179
3	15.0	17.0	1.57	0.397
4	15.2	14.5	1.64	0.334
5	14.2	15.2	1.71	0.324
6	14.3	17.0	1.72	0.360
7	14.1	14.8	1.90	0.342
8	14.6	12.5	2.22	0.269
9	13.8	12.5	3.42	0.189
10	13.8	12.5	4.55	0.253
11	13.5	13.2	7.20	0.467
12	13.7	14.8	9.32	0.726
13	15.7	14.7	12.51	1.17
14	15.6	13.2	17.22	2.04
15	14.8	20.8	1.64	0.381
16	14.8	20.7	1.80	0.347
17	14.6	18.1	2.47	0.290
18	13.5	18.8	4.10	0.264
19	14.2	19.8	4.67	0.292
20	14.0	18.5	5.29	0.331
21	13.8	18.2	6.75	0.436
22	13.5	18.6	9.40	0.710
23	16.3	20.7	12.63	1.15
24	15.2	17.8	17.29	1.99
25	14.5	23.7	1.84	0.378
26	14.8	24.7	2.05	0.360
27	15.0	24.7	2.40	0.324
28	14.8	25.5	2.99	0.318
29	14.7	24.7	3.10	0.277
30	14.0	26.1	3.81	0.300
31	14.7	26.7	4.53	0.334
32	14.0	23.9	4.95	0.316
33	15.6	25.3	6.05	0.415
34	15.0	25.7	8.78	0.634
35	16.8	23.9	12.98	1.16
36	17.5	26.3	13.00	1.15
37	15.6	26.8	16.51	1.72

Table VII (Continued)

Reference No.	Temperature (°C)	Concentration (%)	Mean velocity of mixture (fps)	Head loss (ft. of mixture)/ft
38	14.2	27.5	1.81	0.397
39	15.6	28.1	2.24	0.358
40	15.7	30.5	3.25	0.337
41	14.3	27.9	4.40	0.329
42	14.2	30.0	5.38	0.386
43	13.7	28.3	7.24	0.499
44	13.5	28.7	8.70	0.606
45	16.0	28.2	13.38	1.17
46	16.0	29.7	15.32	1.47

Table VIII

Material: Lead
 Diameter of Particle: 0.0505 in.
 Specific Weight: 705 pcf

Reference No.	Temperature (°C)	Concentration (%)	Mean velocity of mixture (fps)	Head loss (ft. of mixture)/ft
1	3.3	5.5	6.82	0.478
2	3.8	10.0	2.64	0.245
3	5.0	12.5	2.68	0.392
4	4.1	10.0	3.88	0.271
5	1.5	10.2	5.13	0.334
6	1.8	11.2	6.69	0.467
7	3.1	12.4	9.42	0.793
8	4.0	14.7	1.64	0.444
9	2.4	14.0	2.70	0.399
10	4.4	14.2	3.00	0.394
11	1.5	14.0	4.88	0.339
12	1.7	14.2	5.90	0.410
13	1.9	13.3	6.95	0.509
14	1.8	13.4	9.00	0.746
15	4.0	15.2	9.52	0.770
16	4.5	22.0	2.24	0.514
17	2.3	23.5	6.98	0.548
18	13.2	6.3	4.07	0.207
19	12.2	4.5	5.80	0.337
20	13.1	7.2	6.90	0.444
21	12.2	5.5	7.69	0.731
22	12.8	5.6	8.42	0.619
23	14.2	3.1	9.58	0.801
24	14.6	3.6	11.68	1.05
25	14.4	5.4	14.03	1.50
26	14.5	3.5	17.75	2.25
27	15.0	7.6	1.40	0.371
28	13.3	7.9	2.77	0.223
29	12.8	11.7	4.77	0.274
30	12.2	10.0	5.05	0.298
31	12.7	12.1	5.29	0.324
32	13.0	11.5	6.87	0.441
33	12.5	10.3	7.90	0.559
34	12.8	8.6	8.82	0.658
35	16.0	10.5	9.40	0.720

Table VIII (Continued)

Reference No.	Temperature (°C)	Concentration (%)	Mean velocity of mixture (fps)	Head loss (ft. of mixture)/ft
36	13.3	11.2	9.78	0.788
37	14.6	8.0	10.90	0.992
38	15.4	11.2	11.10	0.971
39	14.5	7.8	14.19	1.49
40	15.5	9.8	14.45	1.52
41	14.0	10.5	17.43	2.12
42	14.7	13.8	1.90	0.428
43	13.2	15.3	2.75	0.346
44	12.5	14.7	3.28	0.365
45	12.3	16.0	3.44	0.329
46	14.8	14.1	4.51	0.266
47	12.7	16.2	4.64	0.298
48	20.5	15.6	5.36	0.342
49	20.3	15.3	5.68	0.355
50	12.7	14.2	6.83	0.454
51	12.7	16.3	6.93	0.483
52	12.9	16.3	6.98	0.478
53	12.7	12.9	8.13	0.590
54	12.8	14.7	8.44	0.621
55	12.8	14.7	8.51	0.626
56	14.9	13.5	11.18	1.00
57	15.8	15.3	14.03	1.40
58	15.2	13.0	14.60	1.49
60	14.0	13.3	17.65	2.08
61	13.4	20.7	1.38	0.556
62	13.2	19.0	1.99	0.470
63	12.7	21.8	2.71	0.436
64	12.3	19.7	3.90	0.316
65	12.6	18.2	4.57	0.331
66	12.9	22.4	6.70	0.457
67	12.8	21.7	7.56	0.548
68	12.8	17.8	9.57	0.712
69	15.0	22.2	11.73	1.01
70	14.9	17.7	14.23	1.41
71	14.8	22.1	14.60	1.41
72	14.7	19.8	17.51	2.00
73	15.2	26.2	1.83	0.472
74	13.7	25.5	1.93	0.561
75	12.8	24.6	2.34	0.491
76	12.7	23.6	4.57	0.360
77	12.5	26.4	6.64	0.475
78	12.7	24.1	7.85	0.556

Table VIII (Continued)

Reference No.	Temperature (°C)	Concentration (%)	Mean velocity of mixture (fps)	Head loss (ft. of mixture)/ft
79	12.5	24.8	8.95	0.660
80	13.2	22.5	9.41	0.726
81	14.9	27.2	11.87	0.994
82	14.5	24.4	14.48	1.39
83	14.0	23.1	14.88	1.46
84	14.4	29.5	1.68	0.603
85	14.1	28.9	1.87	0.543
86	13.7	31.4	2.69	0.498
87	13.8	31.4	3.10	0.501
88	13.8	31.9	4.06	0.438
89	13.2	27.9	4.15	0.415
90	12.7	29.3	4.69	0.394
91	13.6	28.6	5.06	0.397
92	12.6	29.7	5.44	0.433
93	14.5	28.6	6.29	0.444
94	12.7	27.9	6.53	0.480
95	13.2	28.2	7.56	0.522
96	12.7	28.3	8.43	0.616
97	13.0	32.0	8.81	0.626
98	12.3	31.1	8.90	0.629
99	14.3	32.0	9.82	0.746
100	14.9	29.2	12.07	1.01
101	15.0	27.8	14.72	1.38
102	15.0	32.4	15.27	1.39
103	14.2	31.2	17.12	1.73
104	14.3	30.6	17.41	1.81
105	15.2	30.7	17.68	1.82
106	15.0	30.3	17.90	1.83
107	14.2	38.4	1.61	0.728
108	14.2	36.5	1.67	0.634
109	12.8	33.6	5.34	0.378
110	14.1	49.7	2.66	0.538
111	13.3	43.6	6.68	0.462
112	12.8	49.0	7.85	0.611
113	13.5	46.7	7.97	0.559
114	13.1	46.0	8.70	0.663
115	12.8	43.0	8.78	0.658
116	14.0	55.3	3.06	0.553
117	13.8	55.0	4.03	0.553
118	15.7	57.5	4.68	0.538
119	13.3	51.7	5.33	0.544
120	13.7	53.3	6.25	0.543

Table VIII (Continued)

Reference No.	Temperature (°C)	Concentration (%)	Mean velocity of mixture (fps)	Head loss (ft. of mixture)/ft
121	13.0	51.2	7.18	0.587
122	13.5	54.5	7.72	0.611
123	13.5	62.5	4.37	0.569
124	14.6	63.8	5.20	0.582
125	13.7	60.0	5.33	0.548
126	13.5	61.6	5.85	0.582
127	29.8	0	5.02	0.227
128	28.3	15.9	3.42	0.386
129	29.5	16.6	4.92	0.300
130	29.7	14.8	5.13	0.308
131	29.4	14.2	5.30	0.311
132	29.7	14.2	5.36	0.311
133	27.7	13.5	6.99	0.428
134	29.0	14.0	9.58	0.676
135	30.2	23.5	5.20	0.339
136	29.6	26.3	5.40	0.363
137	31.0	25.0	7.95	0.530
138	30.2	29.6	1.80	0.579
139	30.2	29.6	3.24	0.470
140	29.3	30.5	3.82	0.444
141	31.0	30.2	5.70	0.418
142	31.0	29.4	6.43	0.441
143	30.2	30.3	8.63	0.587
144	30.3	29.6	9.16	0.626
145	53.7	12.0	3.36	0.261
146	53.7	15.0	2.76	0.418
147	53.7	15.5	2.94	0.365
148	50.5	16.2	3.37	0.410
149	53.9	16.4	4.31	0.253
150	50.9	14.0	4.57	0.274
151	51.2	13.5	4.98	0.277
152	50.5	13.9	6.93	0.378
153	50.8	13.6	7.28	0.420
154	51.0	14.2	9.90	0.658
155	51.9	22.0	2.62	0.491
156	58.8	22.1	2.92	0.449
157	52.1	19.9	3.01	0.441
158	50.4	17.5	9.46	0.613

Table VIII (Continued)

Reference No.	Temperature (°C)	Concentration (%)	Mean velocity of mixture (fps)	Head loss (ft. of mixture)/ft
159	50.5	26.9	2.14	0.480
160	51.0	28.0	2.52	0.522
161	51.0	31.3	3.10	0.499
162	50.3	28.6	4.03	0.384
163	53.0	30.4	4.96	0.376
164	50.3	28.0	4.98	0.363
165	50.8	30.6	6.08	0.407
166	50.5	32.0	7.86	0.506
167	50.5	29.9	9.03	0.585
168	66.0	0	10.50	0.726
169	67.5	11.3	5.08	0.264
170	66.1	14.8	2.70	0.360
171	67.0	17.0	4.79	0.271
172	63.8	17.5	9.76	0.600

Table IX

Material: Sand (Data read from curves of Blatch report)
 Diameter of Particle: 0.02 in.
 Specific Weight: 164.7 pcf
 Temperature: Approximately 13°C

Reference No.	Concentration curve read (%)	Mean velocity of mixture (fps)	Head loss (ft. of mixture)/ft
1	Approximately 12.2	1	0.114
2		2	0.116
3		3	0.118
4		4	0.120
5		5	0.130
6		6	0.162
7		7	0.196
8		8	0.237
9		10	0.326
10		12	0.453
11		14	0.605
12	Approximately 22.7	1	0.190
13		2	0.181
14		3	0.173
15		4	0.164
16		5	0.167
17		6	0.187
18		7	0.216
19		8	0.253
20		10	0.327
21		12	0.458
22		14	0.633
23	Approximately 31.8	1	0.226
24		2	0.218
25		3	0.210
26		4	0.200
27		5	0.203
28		6	0.228
29		7	0.253
30		8	0.279
31		10	0.343
32		11	0.404
33		Approximately 39.8	1
34	2		0.250
35	3		0.243
36	4		0.236
37	5		0.243
38	6		0.266

Table IX (Continued)

Reference No.	Concentration curve read (%)	Mean velocity of mixture (fps)	Head loss (ft. of mix- ture)/ft
39		7	0.285
40		8	0.306
41		9	0.329